geosciences

MDPI

Article

Structural complexity and seismogenesis: the role of the transpressive structures in the 1976 Friuli earthquakes (Eastern Southern Alps, NE Italy)

Giulia Patricelli [1]* and Maria Eliana Poli [1]

[1] Dipartimento di Scienze AgroAlimentari, Ambientali e Animali, Università degli Studi di Udine, Udine (UD), Italy; giulia.patricelli@uniud.it (GP); eliana.poli@uniud.it (MEP)
* Correspondence: giulia.patricelli@uniud.it

Abstract: We reconstructed the seismotectonic setting of the area comprising the northeastern Friuli Plain and the Julian Prealpine border (NE Italy) by integrating geological and seismological data. The study area represents the junction zone between the SSE-verging polyphase thrust-front of the Southalpine Chain and the NW-SE trending strike-slip faults of eastern Friuli-western Slovenia domain. Following a multidisciplinary approach, the 3D –geometry of the Susans-Tricesimo Thrust System was reconstructed through the elaboration of four geological cross sections derived from the interpretation of ENI industrial seismic lines. In a second step, the seismogenic volume of central-eastern Friuli area was investigated through the hypocentral distribution analysis: the seismic events of the latest 50 years (1976–1977- and 1978–2019-time intervals) were plotted on 4 NE-SW oriented seriated sections together with the fault planes geometry. Through this procedure we were able to investigate the relationship between the NW-SE striking high angle faults, which characterize the northern Julian Prealps, and the WSW-verging medium angle reverse fronts located at the piedmont of the Friuli plain, which experienced NW-SE to NNW-SSE oriented compression starting at least from Pliocene. In detail, we examined the involvement of these structures during the seismic sequences of May and September 1976, in terms of activation and/or interaction. The resulting seismotectonic model highlights the interplay between transpressive/strike-slip and reverse planes. In particular, this study suggests that Predjama and Maniaglia transpressive faults strongly control the stress release and likely played a fundamental role both during the May 6th (Mw 6.5) and September 15th (Mw 6.0) Friuli earthquakes.

Keywords: 1976 Friuli earthquakes; inherited structures; slip partitioning; seismogenic segments; eastern Southern Alps; NE Italy.

Citation: Lastname, F.; Lastname, F.; Lastname, F. Title. *Geosciences* **2022**, *12*, x. https://doi.org/10.3390/xxxxx

Academic Editor: Firstname Lastname

Received: date
Accepted: date
Published: date

Publisher's Note: MDPI stays neutral with regard to jurisdictional claims in published maps and institutional affiliations.

Copyright: © 2022 by the authors. Submitted for possible open access publication under the terms and conditions of the Creative Commons Attribution (CC BY) license (https://creativecommons.org/licenses/by/4.0/).

1. Introduction

NE Italy is one of the most seismic regions in the Mediterranean area. In particular, seismicity of Friuli region is mostly concentrated along the Carnian and Julian alpine and pre-alpine arcuate belt (Fig. 1). At present, this area undergoes an about NNW-SSE oriented sigma 1 [1] and the accumulating stress is released through the interaction between the SW-NE to WNW-ESE trending compressional fronts of the eastern Southalpine belt in Friuli [2] and the Dinaric NW-SE strike-slip fault-systems of W-Slovenia [3,4,5,6].

The study area was affected by a polyphase tectonic history: the Mesozoic extensional event was initially followed by the Upper Cretaceous - middle Eocene (External Dinaric chain), and then by the Neogene-Quaternary (eastern Southern Alps) compressional events. The derived tectonic structures, developed under different maximum principal stress (σ1), are characterized by different orientation and gave rise to a complex structural crustal arrangement where the inherited structures were often reactivated by

the ~~latest~~ one. At present, both Mesozoic, Paleogene and Neogene-Quaternary structural systems are affected by the NW-ward propagation of NW-SE trending dextral strike-slip fault-systems of western Slovenia developing since Miocene-Pliocene transition [4].

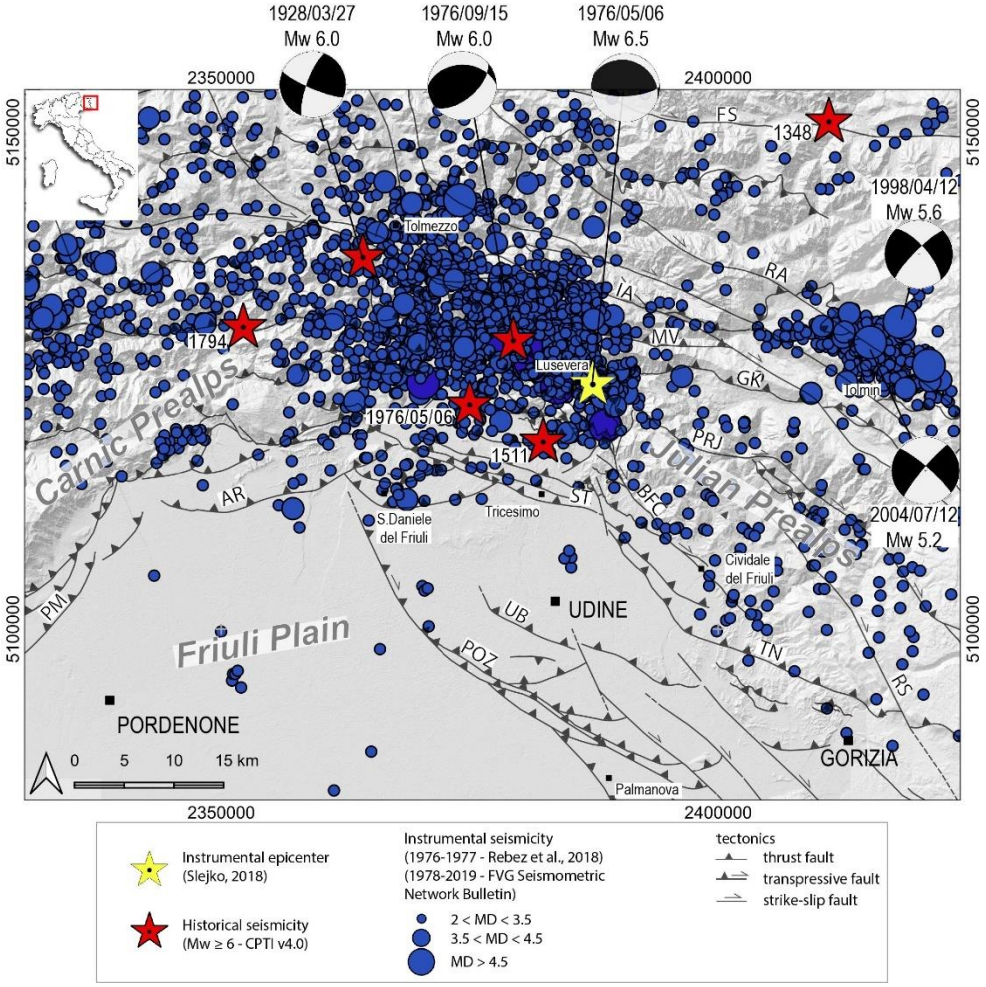

Figure 1. Seismicity of the Friuli region and western Slovenia. Focal mechanisms from [7]. Faults acronyms: AR: Arba-Ragogna Thrust; BFC: Borgo Faris-Cividale Fault; FS: Fella Sava Ft.; GK: Gemona-Kobarid Th.; IA: Idrija-Ampezzo Ft. MV: Musi-Verzegnis Th.; PM: Polcenigo-Maniago Th.; POZ: Pozzuolo Th.; PRJ: Predjama Ft.; RA: Ravne Ft.; RS: Raša Ft.; ST: Susans-Tricesimo Th.; TN: Trnovo Th.; UB: Udine-Buttrio Th.

Aiming at the study of the tectonic structures able to release strong earthquakes, this work focuses on the seismotectonic characterization of the active fault-systems of northern Friuli Plain and southern Julian Prealps. Starting from the interpretation of seismic lines gently supplied by ENI_SpA (henceforth ENI), the 2D and 3D structural setting of the study area was reconstructed by means of 3D-MOVE software, while the seismogenic volume was investigated through the analysis of seismicity distribution, freely available on the CRS-OGS Friuli Venezia Giulia Seismometric Network Bulletin [8]. In order to explore the involvement of the Susans-Tricesimo Thrust-System during the Friuli seismic events, the hypocentral distribution of 1976-77 was analyzed and compared with the post 1977-time interval seismicity. In this context, particular attention was dedicated to the interaction between NW-SE trending high angle faults of the northern Julian Prealps and the WSW verging medium angle reverse planes located in the northern Friuli Plain, which experienced a polyphase tectonic evolution. The obtained data allowed us to formulate new hypotheses regarding the present seismotectonic setting and the seismogenesis of the eastern Friuli area.

2. Geological and seismotectonic setting

The Cenozoic structural framework of NE Italy is the result of the collision and indentation of Adria microplate ~~under the Alpine Chain~~ [9,10]. After the Mesozoic rifting phase, the first compressive event involving the study area was characterized by a NE-SW oriented maximum stress axis, which caused the Upper Cretaceous-middle Eocene SW-ward migration of the External Dinaric fold and thrust belt often through the inversion of the Mesozoic NW-SE striking normal faults [11]. Starting from late Oligocene - early Miocene (Chattian –Burdigalian event in [12]) the northern sector of the eastern Southern Alps (ESA) was affected by exhumation [13,14], but only during the middle Miocene, in response to an about NNW-SSE to NW-SE oriented maximum compressional stress [12,15,16], a S-SE-verging, ENE-WSW fold and thrust belt, coupled with a strongly subsiding slightly N-tilted foredeep [13,17], developed in the Veneto and Friuli Alps and Prealps [18]. In this regard, [19,15,20] highlight the persistence of an alternate NW-SE to NNW-SSE stress regime starting from Messinian to Pliocene ("*twist tectonics*" in [21,16]). In particular, on the basis of detailed analyses of pitted pebbles of the Veneto and Friuli prealpine regions, [16,20] confirm a NNW-SSE main stress tensor also during the early-middle Pleistocene. [19] proposes a NW-SE stress tensor for the Plio-Quaternary time span. As a consequence of the southward propagation of the Southalpine fronts, the inherited Paleogene Dinaric structures were folded, reactivated, and/or dismembered [11,22,23]. Since Miocene-Pliocene transition, the onset of the counterclockwise rotation of Adria microplate [24], combined with its northward motion, resulted in an oblique convergence. As a result of this articulated framework, the structural style gradually changes from West to the East: from thrusting in the Venetian Alps and Prealps [12], to oblique in the Italian-Slovenian border region [23,25,26,27] and then to strike-slip in western Slovenia [28,4,29,30,5,6].

At present, GPS measurements reveal for the Friuli region 2-3 mm/yr of shortening [31,32,33,1], which is absorbed both by NW-SE trending high angle strike-slip structures in the easternmost Friuli area and western Slovenia [5,34,6], and by reverse WSW-ENE to WNW-ESE striking neoalpine frontal ramps in Veneto and Friuli prealpine area [2].

Concerning the seismicity of NE Italy and surroundings, the distribution of fault plane solutions (FPSs) of the major earthquakes [7] registered by the OGS seismometric network [35] suggests that the oblique convergence is still active [3,26,25], in good agreement with the stress and strain tensors of the Friuli and western Slovenian area computed through the inversion of focal mechanisms by [36]. Seismicity depicts an arcuate belt coinciding with the alpine and pre-alpine border region of Friuli Venezia Giulia and western Slovenia (Fig. 1). Particularly, focusing on the historical seismicity (from the Parametric Catalogue of Italian Earthquakes, CPTI15 v4.0) [37], two destructive seismic events (Mw ≥ 6.0) are documented within the Julian Prealpine area since the year 1000: the 1511 and the 1976 earthquakes. Regarding the 1511 event, on March the 26th a strong earthquake (Mw 6.3) affected a wide area extending from Friuli to western Slovenia. Based on the updated macroseismic field elaborated by [38], the revised epicenter has been located near Tarcento, where Io 9 MSC was estimated. On the contrary, CFTI5 MED [39] reports two strong events during March and August 1511. The macroseismic epicenter of the first 1511 earthquake (equivalent magnitude Meq 7) is located near Montefosca, in the Natisone valley, while a subsequent event (Meq 6) is documented on the August the 8th 1511 near Banjšice, in western Slovenia. Concerning the possible source responsible of the 1511 events, it is worth noting that both March and August macroseismic epicenters from CFTI5 MED are located on the Predjama strike-slip Fault. Based on macroseismic data inversion, [40] proposed an earthquake-model scenario consistent with a Mw 6.9 event which activated the 50 km long SE portion of the Idrija strike-slip Fault. Differently, as already suggested by [41,38] concluded that the 1511 earthquake involved both Alpine and Dinaric structures.

Recent paleoseismological analyses on the NW-SE strike slip fault-system of the eastern Italy and western Slovenia, revealed Holocene surface rupturing referable to the 1511

event across the Colle Villano – Borgo Faris-Cividale Fault System [26], across the Idrija [42,34] and Predjama Faults [34].

The more recent 1976 Friuli sequences have been accurately described and analyzed by [43] based on a large amount of bibliography. Preceded by a Ml 4.5 foreshock, a destructive earthquake (on May the 6th 1976, Ml 6.4) struck central-eastern Friuli, where Imax 9-10 MSC was recorded. After the strong Ml 5.3 aftershock on May the 9th 1976, seismic activity slowly decreased until September 1976. Two quakes on September the 11th 1976 (Ml 5.1 and 5.6, respectively) and two others on September the 15th 1976 (Ml 5.8 and 6.1, respectively) caused further damage. One year later, on September the 16th 1977, another seismic event with Ml 5.2 occurred and was followed by its aftershock series which lasted more than one month. The only data interpreted as coseismic deformation [44] come from topographic leveling measurements done in 1952 and [45]. The new leveling made by Udine University and Civil Defense of FVG Region [46] in 1997 demonstrated that the estimated 25 cm of maximum deformation between Venzone (+ 18 cm) and Carnia (-7 cm) localities were a coseismic deformation. Regarding the Mw 6.5 mainshock, the macroseismic epicenter is located between Buia and Gemona del Friuli (Fig. 1, [37]), while the instrumental location of the event [43] is placed near Lusevera, about 12 km ENE, in a sector of the Julian Prealps where no major settlements are found. Regarding the focal mechanism of the mainshock of May most of the available interpretations agree for the activation of a reverse N-dipping low angle plane [7], with only a small oblique component. Differently, concerning the focal mechanism solution of the strongest event of September the 15th (Ml 6.1) different interpretations are present in the literature [7], which mainly propose the activation of a reverse N-dipping plane or of a NNE-dipping reverse-oblique geometry.

Regarding the possible source, most of the interpretations agree with the activation of two different structures. [47] proposed the activation of the Buja-Tricesimo Fault for the May event and the involvement of the Periadriatic Thrust (or Barcis-Staro Stelo *Auct.*) during September. [48] on the basis of hypocenters relocation, long period surface wave inversion, field geology and strong motion modelling revisited the 1976 Friuli earthquake sequence and proposed that the Friuli earthquake rupture was related to a 19 km fault-related folding evolving from blind faulting beneath the Bernadia and Buia basement-involved structures to semi-blind faulting beneath the Susans structure. On the basis of geological and seismological evidence [49,2] proposed the activation of the Susans-Tricesimo Thrust for the May event and assessed the activation of a deeper blind structure during the event of September. The activation of a single source for the entire sequence, whose surficial expression is compatible with the Buia-Tricesimo Thrust, was proposed by [33] based on geodetic data. Conversely, [50] attributed most of the events to the Periadriatic Overthrust and only two aftershocks of May to the inherited Dinaric structures. Recently, [25] confirmed the Susans-Tricesimo Thrust as the responsible source of the May event, based on the evidence of Quaternary deformation both on the surface and in seismic ENI profiles and the possible activation of the Buia Thrust was not excluded. Following the 1976-1977 sequence, the instrumental seismicity recorded two other more recent seismic events in 1998 and 2004 (Fig. 1). The April 1998 sequence (Bovec earthquake) had Mw 5.6 [51,52,53], while Mw 5.2 event was registered during the July 2004 (Tolmin earthquake) [54]. Both sequences are associated to the NW-SE dextral strike-slip Ravne Fault, which is actively propagating through interaction of individual right-stepping fault segments and breaching of local transtensional step-over zones [52,29].

3. Methodology

3.1. Structural model reconstruction

The interpretation of a grid of ENI seismic lines of the northern Friuli Plain allowed to reconstruct the buried structural setting of the study area. Four of the analyzed seismic

profiles have been selected for the construction of the bi-dimensional and tri-dimensional model of the area.

Starting from the upper Carnian Travenanzes Formation, the simplified stratigraphic model of Friuli region, functional to the interpretation of seismic lines, is composed of five seismo-stratigraphic units [55,17].

- The Mesozoic platforms succession includes the Dolomia Principale and the Friuli-Dinaric carbonate Platform [23], which developed from late Triassic to middle-late Cretaceous. It is composed of an about 3000 m thick sequence of platform facies, with locally transgressive and emersion episodes [56,57,58,59,60].
- The Upper Cretaceous-Middle Eocene turbiditic sequence represents the filling of the foredeep of the SW-verging External Dinaric Chain. The complete westward thinning sequence up to 4000 m [61,13] is characterized by siliciclastic turbiditic sequence (Campanian-Maastrichtian flysch), carbonatic megabeds (*seismoturbidites* [62]) (Grivò Flysch, Thanetian *p.p.* – Ypresian *p.p.*) and calciclastic and siliciclastic turbidites in the upper part (Savorgnano Marls and Arenites and Cormons Flysch, lower-middle Eocene) [63,64,65,66].
- The lower-middle Miocene sequence is commonly referred as "Cavanella Group" and is composed of shallow water marine sediments [67,18,68,13]. In the context of seismic lines interpretation, Cavanella Group represents an important regional-scale seismo-stratigraphic group of reflectors, showing an overall tabular geometry and a SW-ward thinning with thicknesses spanning from hundreds to tens of meters [17].
- The middle to upper Miocene Molasse sequence represents the foredeep deposition of the SE-ward verging and migrating Southalpine Chain. In the Piedmont Friuli Plain, at the outer border of the prealpine relieves, the upper portion of the sequence consists of very thick fan delta and alluvial deposits dated back to latest Tortonian-early Messinian (Montello Conglomerate, [66,69]), testifying the transition from terrigenous platform to continental facies [18,23].
- The Plio-Quaternary sequence develops on top of the Messinian Unconformity. It is composed of thick conglomeratic channel bodies filling the narrow Messinian canyons since the successive transgression episode [23,70]. The sea ingression extended in the Tagliamento paleovalley area, north up to Osoppo, where coarse-grained Gilbert-type deltaic bodies are preserved: the Osoppo Conglomerate, dated back to Zanclean [20,71]. The middle-to-late Pleistocene sequence covering the erosional plain surface includes alluvial and glacial facies [66,69,23,70].

A simplified seismostratigraphic model was elaborated (Table 1) for the 2D time to depth conversion by integrating the stratigraphic framework of the study area with the velocity logs of some ENI exploratory wells and velocity values extracted from bibliography, in analogy with [27].

Table 1. Velocity model adopted for the 2D depth seismic lines conversion. Velocity values (p-waves) derive from Cargnacco 1, Amanda 1, Gemona1 ENI well-logs and from bibliography [23,17].

Seismostratigraphic unit		Velocity p-waves [m/s]
Plio-Quaternary Units		**2000**
Middle-Upper Miocene Molasse		**3000**
Lower Miocene Cavanella Group		**4000**
Paleogene turbiditic Units		**3600**
Lower Jurassic-Upper Cretaceous Carbonate platform Units		**6100**

Particularly, velocity values of the Jurassic-Cretaceous carbonate platform, late Paleogene - early Eocene turbidites) derived from the Cargnacco 1 and Amanda 1 wells; the middle – late Miocene Molasse velocity derived from Gemona 1 well, while the early - middle Miocene Cavanella Group and Plio-Quaternary succession velocity values were extracted from bibliography [66,69,23,17].

The elaborated velocity model was uploaded in the 3D Move Software, where the interpretation of seismic lines was made. The detected seismostratigraphic tops (top Cretaceous carbonatic platform, top turbiditic units and top Cavanella Group) and tectonic structures were digitalized on the selected ENI seismic profiles (sections AA' to DD', see traces in Fig. 2). For mapping the Messinian Unconformity, we also consulted the regional database of geognostic wells gently supplied by the Friuli Venezia Giulia Region. The horizon digitalization was driven by the point data of pre-Quaternary bedrock depth, extracted from projected geognostic wells.

Once digitalized, each section was converted from time to depth through the *Database Method* of *2D Conversion* tool, which considers the velocity values settled in the stratigraphic model and compute the conversion procedure as the incremental sum of the thicknesses of equal velocity. Starting from the 2D geological sections obtained from the interpretation of seismic lines, the 3D surface of the main tectonic structure was constructed through the interpolation procedure of the *Create new fault* within the *Create Surface with Boundaries* tool. The C*ontrol Points for Kriging* option was ticked in order to create a surface from points that is geostatistically valid.

3.2. Seismicity distribution analysis

The seismogenic thickness of the studied area was reconstructed through the hypocentral distribution analysis of instrumental seismicity. Two distinct databases were created, referring to the 1976-1977 and 1978-2019 time-intervals. The 1976-77 database includes the complete relocation of the sequence performed by [72] and the latest location of the mainshock epicenter elaborated by [43]. In this context, an update of the North-Eastern Italy Seismic Network catalogue was performed by [73], which revised and corrected magnitude estimation thanks to new linear empirical regressions between Ml and Md for eastern Southern Alps. Differently, the 1978-2019 seismic database contains the events registered by the CRS - OGS Seismometric Network and freely available on the Friuli Venezia Giulia Seismometric Network Bulletin [8]. Both databases were filtered following three criteria: gap < 180°; vertical and horizontal error < 4 km and Md ≥ 1. In this regard, the error distribution analysis shows that among the collected events less than 6 % of the earthquakes have an error comprised between 3-4 km and specifically, they include events with magnitude lower than 3.5.

Focusing on the earthquakes distribution analysis, the events of both databases were classified based on depth and magnitude classes and the 2D depth distribution was analyzed in terms of number of events per depth class. The 1976-77 seismicity was further categorized in three "*time classes*" (May-Aug. 1976; Sept.-Dec. 1976; Jan. – Dec. 1977), in order to analyze the evolution of the sequences with time.

Regarding the 1978-2019 database, the Md values were firstly converted in Ml through the [74] relation and then the corresponding energy value was calculated through the [75] formula, valid for Ml < 4.5 earthquakes. Differently, the [76] relation for strong earthquakes was used for the only Ml 4.9 event. The total released energy per depth class distribution was then analyzed, differentiating by magnitude value. Successively, the epicentral distribution of the earthquakes of both databases was analyzed by plotting the events in map view. In detail, they were categorized in three depth classes (0-7 km; 7-13 km and > 13 km). In a third step, the 3D distribution of the earthquakes was analyzed with respect to the reconstructed fault surfaces by plotting seismicity on seriated sections. Particularly, four N40° trending sections were elaborated, characterized by a length of 30 km, a spacing of 5 km and a projection distance of the events of 3 km.

The focal mechanisms available from the Catalogue of earthquakes of Southern Alps and surroundings area from 1928 to 2019 [7] were consulted for both databases (1976-1977 and 1978-2019). Following the recent focal mechanisms dataset revision, performed by [7], the Catalogue contains all the available focal mechanisms obtained by different Authors and the preferred solution for each event is suggested by the catalogue's Authors.

4.Results

4.1. 3D reconstruction of the Susans-Tricesimo Thrust System

The subsurface geometry of the Piedmont Friuli Plain was reconstructed through the elaboration of four geological cross sections (AA', BB', CC' and DD' in Fig. 2) obtained by the interpretation of the seismic lines gently supplied by ENI (Figs. 3 and 4). The analysis focused on the area between Buia, San Daniele and Tricesimo towns, located into the morainic arc of the Tagliamento river in the central Friuli. It is worth noting that the distribution of seismic lines in the study area is not homogeneous (Fig. 2) preventing the complete interpretation of the lateral continuity of the tectonic structures.

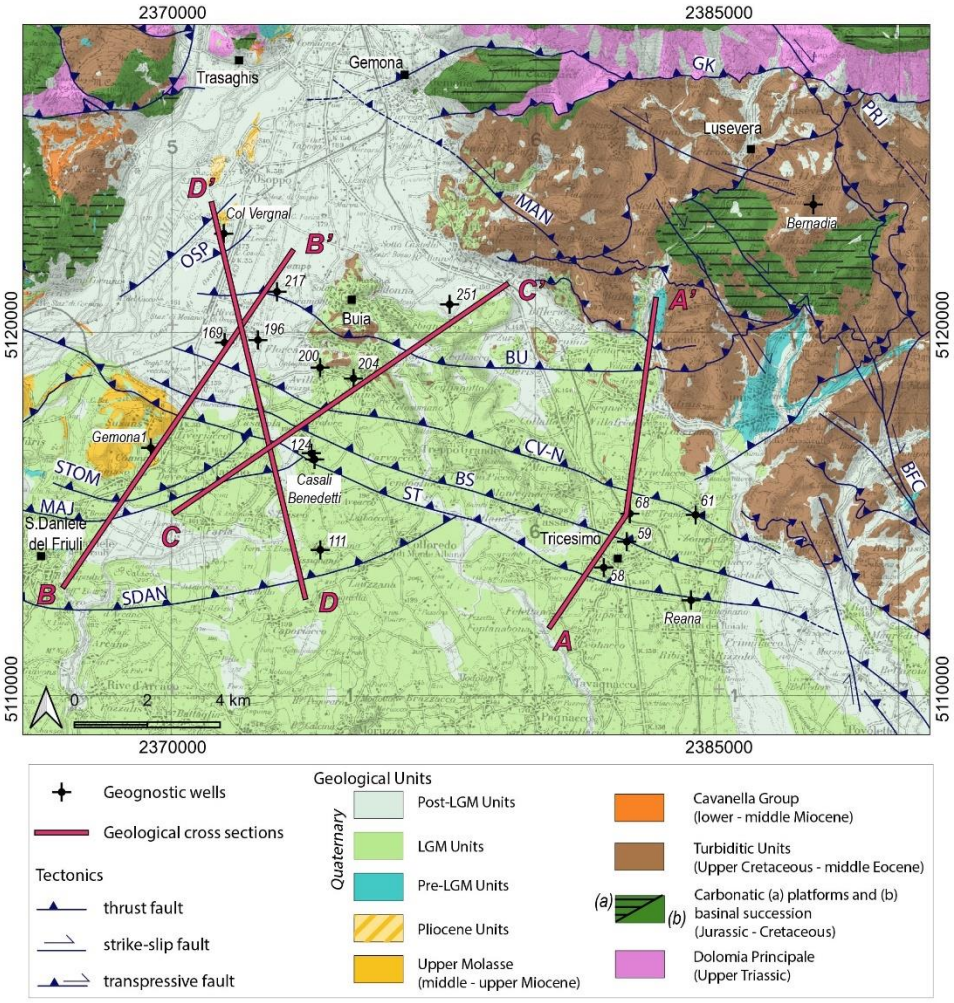

Figure 2. Geological map of the study area (from CARG Geological Sheets 049 Gemona del Friuli and 066 Udine). AA', BB', CC', DD' traces of the geological cross sections elaborated from the interpretation of ENI seismic lines and geognostic wells. Legend: BFC: Borgo Faris-Cividale Faultt.; BS: Borgo Soima Thrust; BU: Buia Th.; CV-N: Colle Villano-North Th.; GK: Gemona-Kobarid Th.; MAJ: Majano Th.; MAN: Maniaglia Ft.; OSP: Osoppo Th.; PRJ: Predjama Ft; SDAN: San Daniele Th., ST: Susans-Tricesimo Th., STOM: S.Tomaso Th.

Particularly, we detected a S-SW verging, WNW-ESE striking thrust-system (the Susans-Tricesimo Thrust System – STTS), composed by a set of reverse faults named Susans-Tricesimo (ST), Borgo Soima (BS) and Colle Villano-North (CV-N), respectively (Fig. 2). The major frontal structure (i.e. the master fault) is the Susans-Tricesimo Thrust, a medium angle thrust that shows a long polyphase tectonic history [47,77,2,25]. ST gives rise to an about 1.2 s displacement of the top of the carbonatic platform and displaces the Cavanella Group of about 0.8 s (Fig. 3 A, B, C, D), indicating that ST was involved in two deformational events (i.e. the Paleogene Dinaric and the Neogene Neoalpine tectonic phases, respectively) after the Mesozoic carbonate platform deposition. Moreover, the reduced thickness of the Serravallian-Messinian Molasse at the hanging wall of ST confirms the Neoalpine activity of the thrust fault, suggesting a syn-depositional growth.

At the hanging wall of ST Thrust, Borgo Soima (BS) and Colle Villano-North (CV-N) Thrust-splays slightly displace the top of the carbonatic platform and can be traced up to the 0 masl.

Concerning the Quaternary units, the interpretation of seismic lines allowed us to decipher that STTS clearly affects the Plio-Quaternary succession suggesting a recent tectonic activity for the whole Thrust-System. In particular, in section AA′ (Fig. 3A), the projected Reana well reaches the top of Upper Molasse at a depth of-260 masl, covered by an about 330 m thick conglomeratic unit (pre-LGM unit) and a 78 m thick gravel deposition (LGM unit). Conversely, about 5 km NW, the n. 61 well testifies the presence of 40 m thick gravel deposition directly above the turbiditic units (encountered at about 140 masl). In addition, in section AA′ (Fig. 3A), BS propagates within a deep Plio-Quaternary paleochannel, probably causing the deformation of the channel itself (Fig. 4A).

The most internal structure detected is the Buia Thrust (BU), a low angle thrust fault which slightly displaces the top of the carbonatic platform. In section AA′ (Fig. 3A) BU is constrained at surface by the tectonic contact between Cavanella Group and Eocene turbidites cropping out near Tarcento [78,23].

In the most internal portion of section DD′ (Fig. 3D) an additional low angle infra-Molasse reverse structure is present: the SE verging, WSW-ENE trending Osoppo Thrust (OSP). This area is constrained by the close Col Vergnal relief and by the homonymous geognostic well located about 250 m South. The relief is formed by Pliocene units (Osoppo conglomerates, [20,79,71,23]), on top of which the presence of LGM deposits (Spilimbergo Synthem - SPB) is documented. Conversely, the Col Vergnal well stratigraphy is characterized by about 30 m Holocene deposits and 60 m LGM units, which lie on top of the upper Tortonian – lower Messinian sandstone-mudstone member of Montello conglomerate (MON2), at 83 masl [23].

In the western portion of the investigated area, at the footwall of ST, three minor reverse faults (about E-W striking) were detected: the San Tomaso (STOM), Majano (MAJ) and San Daniele (SDAN) Thrusts. Particularly, in section CC′ (Fig. 3C) STOM gives rise to a well-developed anticline that involves the Southalpine Molasse and propagates toward the surface, also affecting the bottom of the Quaternary succession (Fig. 4B). Conversely, MAJ and SDAN are characterized by a low angle geometry, running in flat within the Upper Molasse. Majano, San Tomaso and San Daniele Thrusts seem to affect only slightly the Quaternary deposition in this area. Conversely, a clear Quaternary activity can be assessed for ST, BS, CV-N and BU Thrusts.

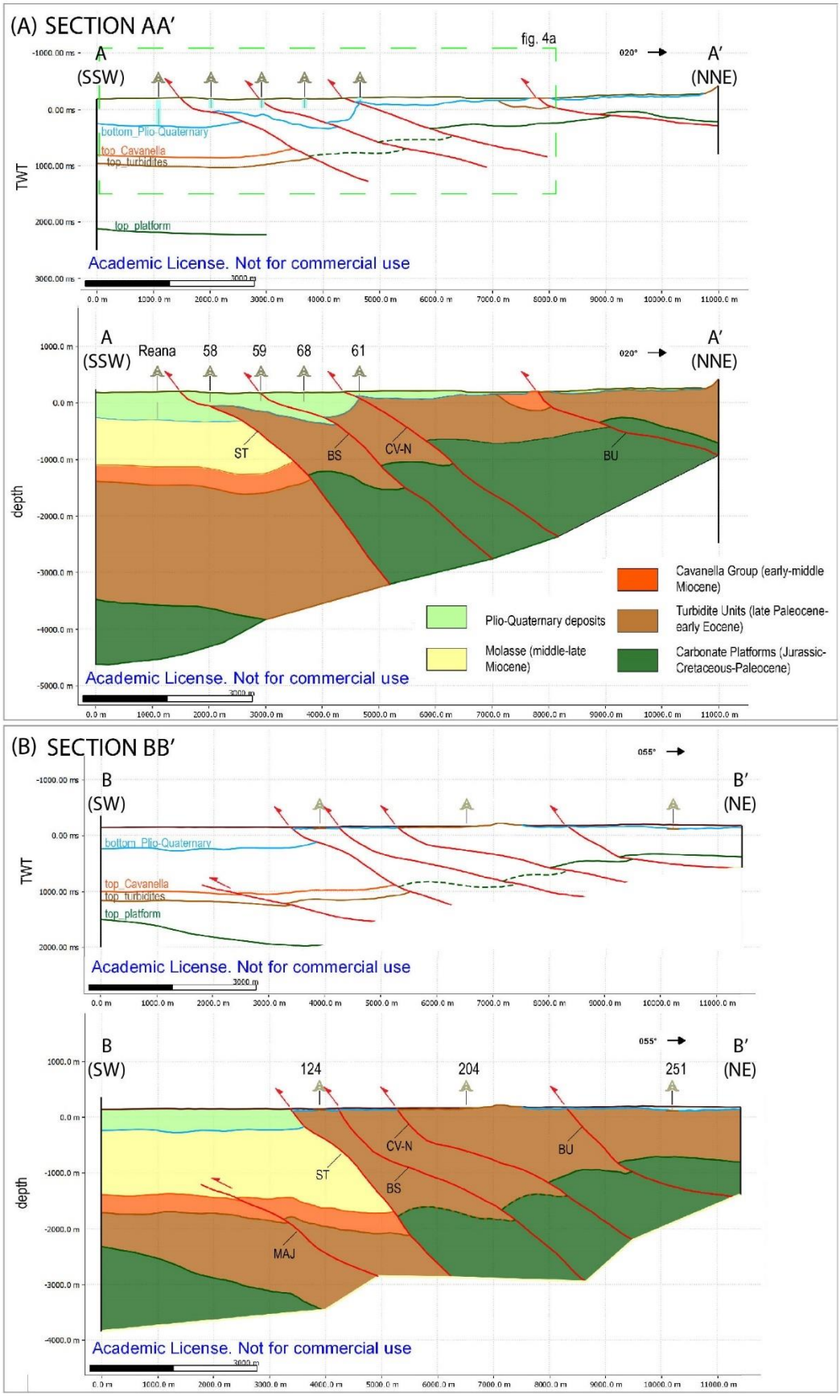

Figure 3. Seismic interpretation of the main seismo-stratigraphic horizon and related geological cross sections AA′ (A), BB′ (B), CC′ (C) and DD′ (D), representing the buried setting of the Piedmont Friuli Plain. Section traces and acronyms are reported in Fig. 2.

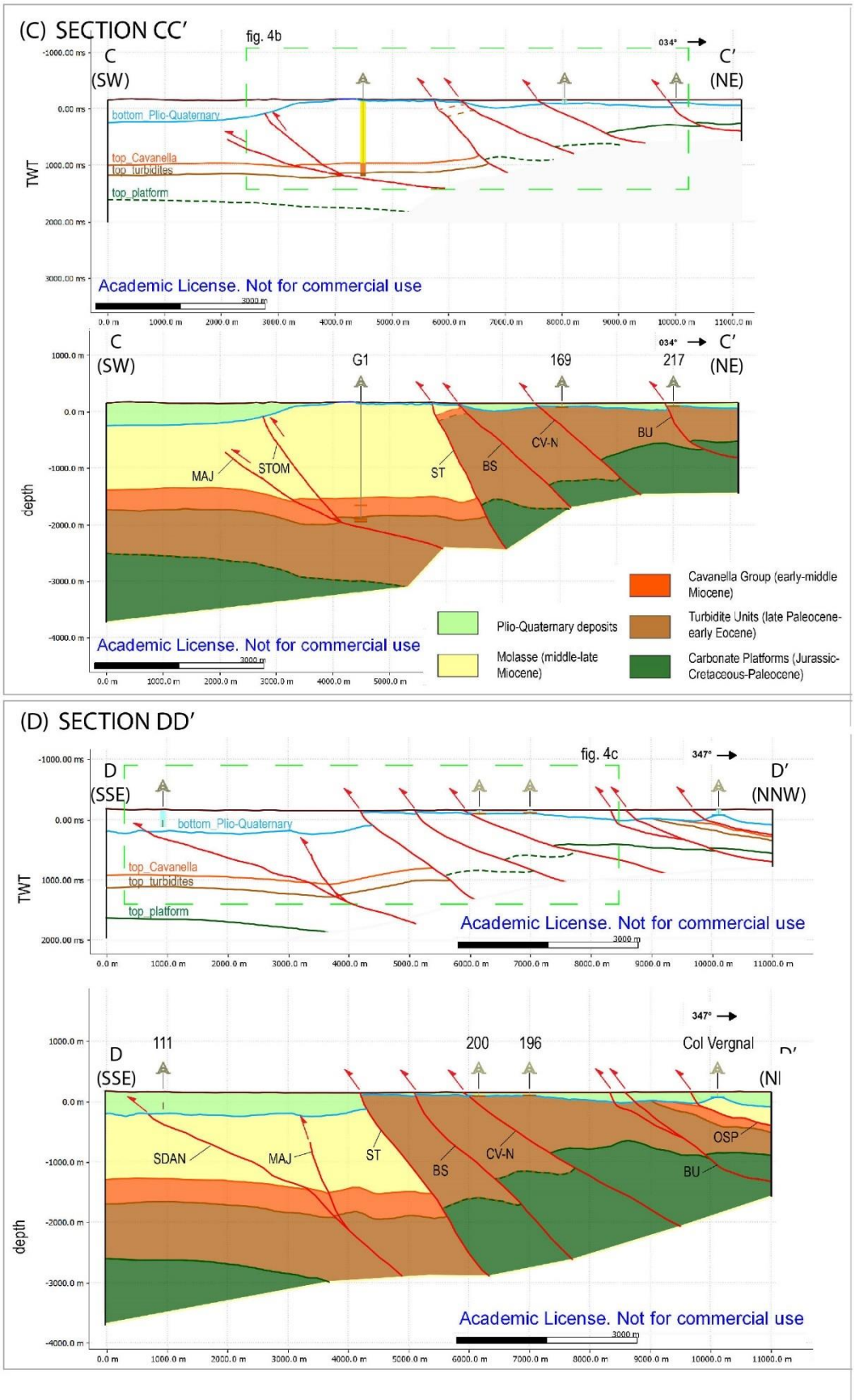

Figure 3 continued.

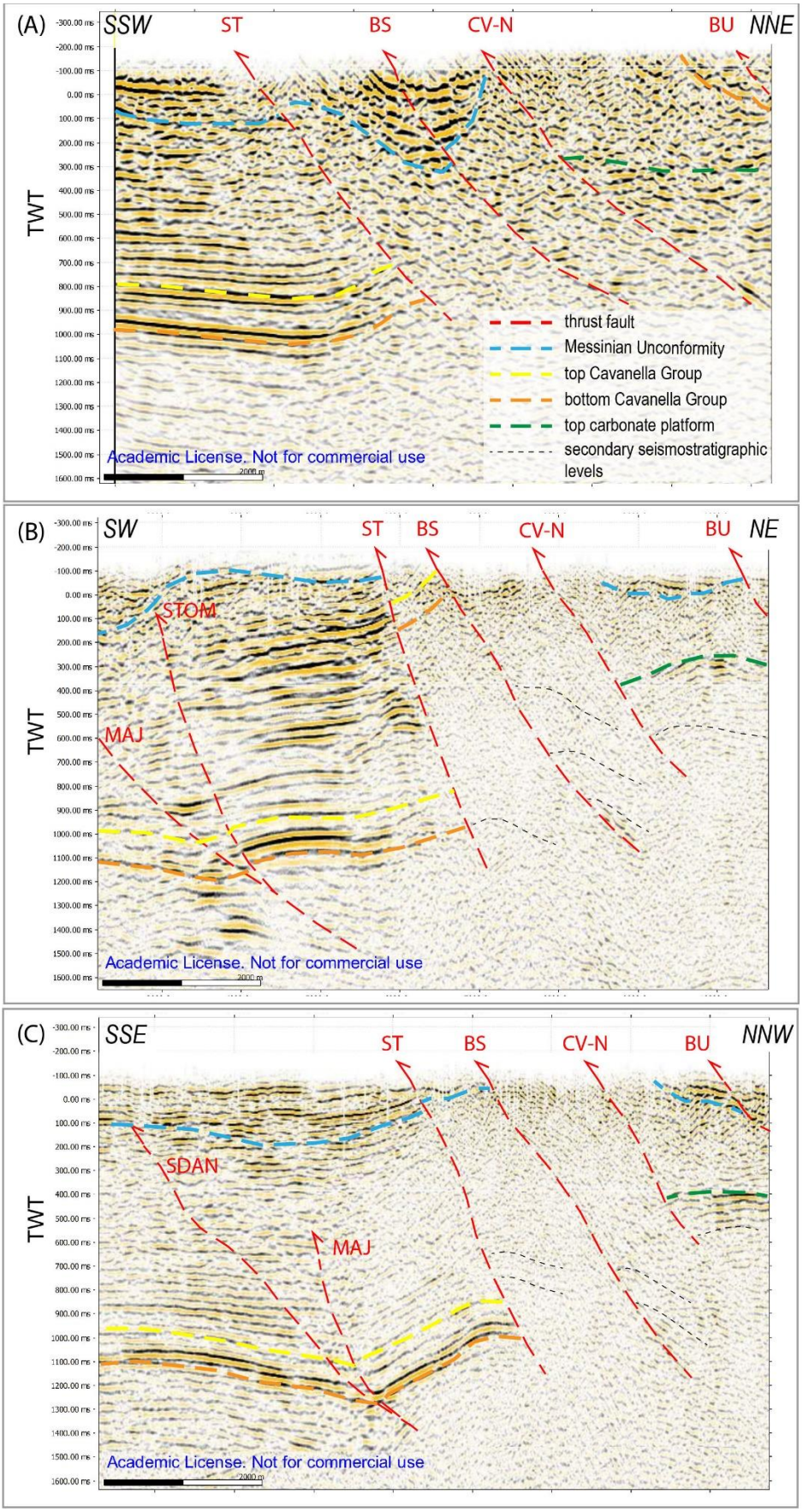

Figure 4. Interpretation of clippings of seismic lines of sections AA′ (A), CC′(B) and DD′ (C) across the Susans-Tricesimo Thrust System, with a 3X vertical exaggeration of the z scale.

Following the elaboration of the geological cross sections, the 2D profiles were interpolated with the aim to reconstruct the 3D geometry of the active Susans-Tricesimo Thrust-System and Buia Th. in the piedmont Friuli Plain. (Fig. 5). It is worth noting that seismic lines allow to reconstruct the geometry of the tectonic structures only in their shallowest portion, ~~deep~~ up to 5 km depth.

In particular, STTS is made by a set of three sub-parallel 40°-45° NNE dipping, WNW-ESE striking reverse faults, arranged in *domes and basins* type structures [80], according to their polyphase tectonic history. We consider the ST Thrust as the master fault, while Borgo Soima and Colle Villano-North represent two minor splays. Conversely, we consider the Buia Thrust as a different structure because it has a different surface strike, and it is characterized by a very low angle dipping geometry (10-20°) in the first 2-3 km depth.

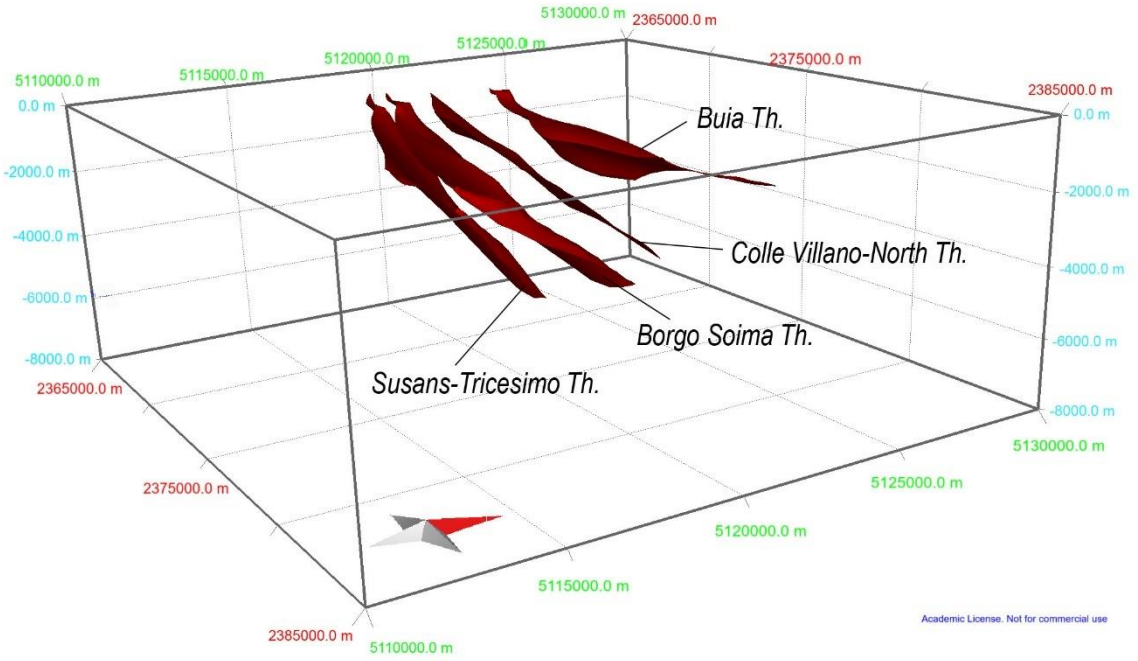

Figure 5. 3D structural model of the Susans-Tricesimo Thrust-System and Buia Thrust, obtained through the interpretation of ENI seismic lines in 3D Move in the first five km.

4.2. Analysis of seismicity distribution

With the aim to make some attempts regarding the investigated tectonic structures as possible sources of the 1976-1977 earthquakes, we analyzed the events collected from 1976 to 2019. Moreover, in order to study the evolution of the seismicity of the Julian Alps and Prealps during the last 50 years, seismicity was divided into two different time intervals: 1976-1977 and 1978-2019. The seismicity distribution was analyzed with respect to the tectonic structures characterizing the study area through the elaboration of four NE-SW seriated sections (traces in Fig. 6). The collected events were plotted together with the active faults of the area, partly reconstructed in this study, and partly extracted from the literature [23,66,69,27]. The strain pattern of the studied fault surfaces was also investigated through the analysis of the available focal mechanisms [7]. Particularly, in order to better define the transpressive, rather than pure dip-slip character of the investigated faults, a special regard was dedicated to the events characterized by an oblique component (Reverse-to Strike-Slip: R-SS; Strike-Slip-to-Reverse: SS-R and Strike-Slip: SS, as in Tables 2 and 3 and Figs. 8, 9, 12). The analyzed events of both 1976-1977 and 1978-2019 seismic databases are identified with a progressive number, listed in Tables 2 and 3, and classified with different colors based on their kinematics.

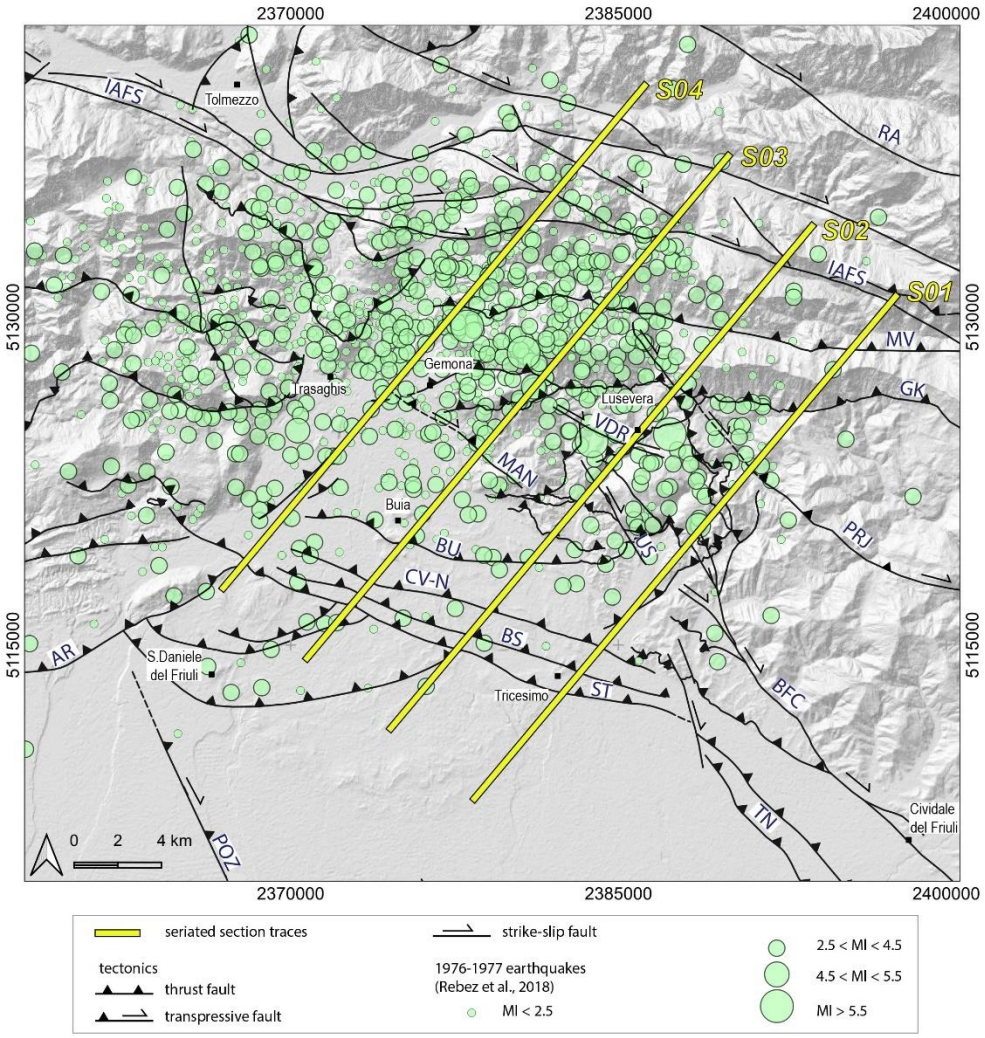

Figure 6. Earthquakes localization from [72] of the 1976-1977 sequences and traces of the seriated sections realized for the 3D distribution analysis of seismicity. Faults acronyms: AR: Arba-Ragogna Thrust, BFC: Borgo Faris-Cividale Fault; BS: Borgo Soima Th.; BU: Buia Th.; CV-N: Colle Villano-North Th.; GK: Gemona-Kobarid Th.; IAFS: Idrija-Ampezzo Ft. System; MAN: Maniaglia Ft.; MV: Musi-Verzegnis Th.; POZ: Pozzuolo Th.; PRJ: Predjama Ft.; RA: Ravne Ft.; ST: Susans-Tricesimo Th.; TN: Trnovo Th.; VDR: Vedronza Ft.; US: Useunt Ft.

4.2.1. 1976-1977 seismicity distribution

First, we analyzed the 1976-1977 sequence relocalized by [72]. With the aim to investigate the spatial evolution of the sequence in time, the collected events were classified in 3 different "*time classes*": May-August 1976, September-December 1976 and January-December 1977 (Fig. 7). This aspect is also useful to explore the possibility that the sequences ruptured one single structure or whether many different sources activated.

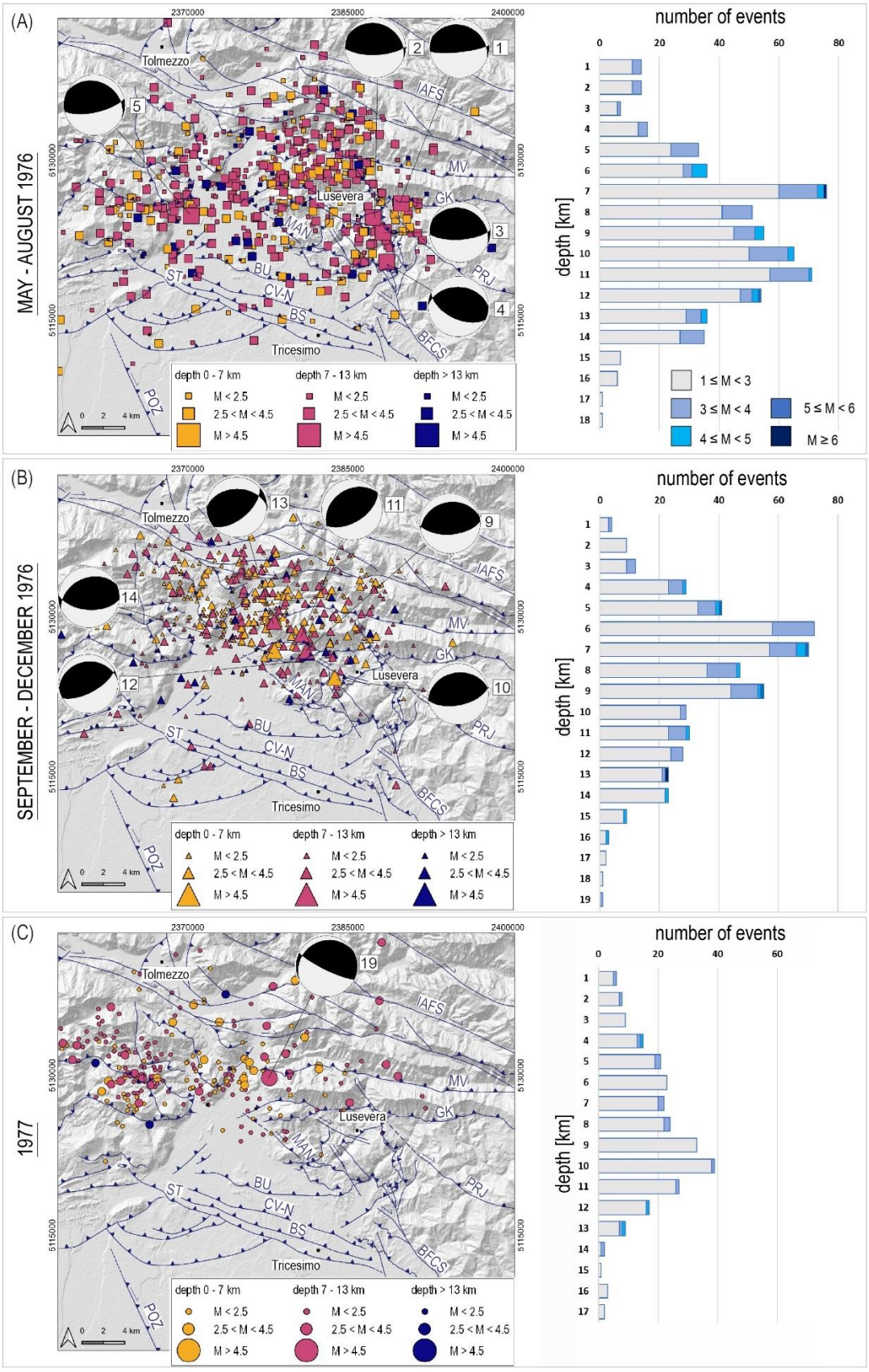

Figure 7. Map and depth distribution of the 1976-1977-time interval seismicity: (A) May-August 1976; (B) September-December 1976; (C) 1977. The number of the events refers to Table 2 and focal mechanisms from [81]. The frequency histograms are in terms of number of events, differentiated per magnitude classes, per depth classes.

Table 2. Collection of analyzed focal mechanisms of the strongest events of the 1976-1977 seismicity. FT refers to the fault type classification by [82], as indicated in [7].

	EVENT PARAMETERS [72]			**Focal Mechanism** [7]		
ID	**DATE**	**TIME**	**DEPTH [km]**	**Ml**	**FT**	**REF**
1	06/05/1976	19:59	9.4	4.5	R	[81]
2	06/05/1976	20:00	7	6.4	R	[81]
3	07/05/1976	00:23	8.5	4.5	R	[81]
4	09/05/1976	00:53	11.6	5.3	R	[81]
5	11/05/1976	22:44	12.0	4.8	R	[81]
6	07/05/1976	11:15	11.7	3.5	R-SS	[49]
7	15/05/1976	16:50	10.2	3	SS	[49]
8	26/06/1976	11:13	5.9	4.3	R-SS	[81]
9	11/09/1976	16:31	8.9	5.1	R	[81]
10	11/09/1976	16:35	4.8	5.4	R	[81]
11	15/09/1976	03:15	7	5.8	R	[81]
12	15/09/1976	04:38	14	4.7	R	[81]
13	15/09/1976	09:21	12	6.1	R-SS	[81]
14	15/09/1976	11:11	6.2	4.5	R	[81]
15	15/09/1976	20:34	5.4	3.7	R-SS	[49]
16	27/10/1976	04:25	5.1	3.3	R-SS	[49]
17	20/11/1976	00:01	5.8	2.9	R-SS	[49]
18	07/12/1976	03:37	7.4	3.6	R-SS	[49]
19	03/04/1977	03:18	12.2	4.5	R	[81]
20	24/08/1977	12:00	6.8	3.4	SS-R	[81]

The maps of Fig. 7 highlight the northwestward migration of the sequences, as already remarked by many Authors [83,84,85,86,43]. However, it should be noted that already during the first sequence (May-August 1976) most of the seismicity is confined to the NW portion of the study area (Fig. 7A).

The depth frequency histogram for each of the three "*time classes*" shows that most of seismicity occurred during the first year. Particularly, the comparison between the two 1976-time classes shows that the mainshock of May-Aug 1976 (Ml 6.4) is located at 7 km depth, which is the most active depth class, while during Sept-Dec 1976 the most active thickness lies between 6 and 9 km depth, but the strongest event of September (Ml 6.1) occurred at greater depth (12 km).

Concerning the focal mechanisms of the strongest events, [81] assessed that the May earthquakes activated a low-to-medium NNE-dipping plane, while the events of September are referable to an E-W trending gently N-dipping geometry (Fig. 7A and B). In this regard, it is worth to note that both [87,88] agreed for a different interpretation of the strongest event of September the 15th (Ml 6.1), proposing the activation of an about NW-SE oriented medium angle plane.

In order to make some attempts regarding possible association earthquake-structure, the distribution of 1976-1977 sequence was analyzed with respect to the tectonic structures of the area. It must be remarked that we interpret the Colle Villano-North (CV-N) and Borgo Soima (BS) Thrusts as secondary splays of the Susans-Tricesimo Thrust System (STTS), then we henceforth refer to the Susans-Tricesimo masterfault (ST) as for the whole structure. The 1976-1977 earthquakes, classified per "*time classes*", and plotted on the seriated sections (Fig. 8, see traces in Fig. 6), reveal a diffuse distribution affecting the whole seismogenic thickness.

Focusing on May-Aug 1976-time interval (Fig. 8, sections 1-4) we observe that at depth seismicity is always confined by means of a frontal medium angle surface, probably referable to the Pozzuolo Thrust System (POZ), i.e. the inherited NW-SE striking, SW-verging frontal thrust of the External Dinaric in Friuli [89], reactivated with oblique component under the Neolpine maximum stress tensor. In the Piedmont Friuli Plain under Udine locality, POZ shows a transpressional

component on the NW-SE striking plane and a pure dip-slip movement on the ENE-WSW striking lateral ramp of Terenzano Thrust, deforming the pre-LGM conglomerates (Friuli Supersynthem) and the LGM surface [90,66,27].

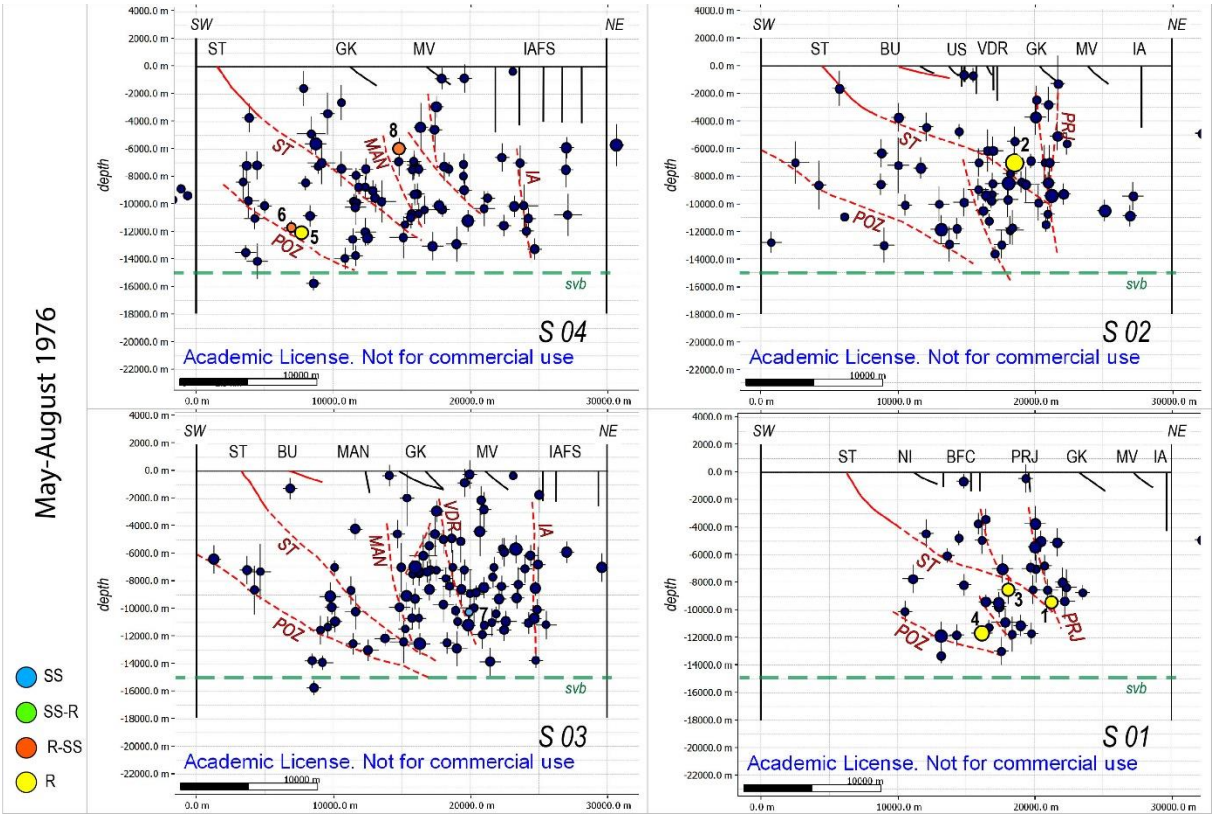

Figure 8. May - August 1976 Ml ≥ 2.5 seismicity plotted on the seriated sections 01, 02, 03, 04 (see traces in Fig. 6) together with the active faults surfaces reconstructed in this study (red thrusts) and tectonic structures known from the literature (black faults, [23]). The symbols size is proportional to the magnitude value (Ml), the number of the events refers to Table 2, while the color refers to the kinematics as shown in the legend. The vertical and horizontal bars for each event represent the vertical (Z) and horizontal (H) error localization, respectively. The red dashed lines refer to the interpretations of the activated structures, recognized on each section. The green dashed line represents the base of the seismogenic volume (svb). Faults acronyms: BFC: Borgo Faris – Cividale Fault-System; BU: Buia Thrust; GK: Gemona-Kobarid Th.; IAFS: Idrija-Ampezzo Ft. System; MV: Musi-Verzegnis Th.; PRJ: Predjama Ft.; ST: Susans-Tricesimo Th.; VDR: Vedronza Fault; US: Useunt Ft.

Towards the NE, seismicity is confined by means of high angle structures. Looking at section 1, located in the south-easternmost edge of the study area, a sub-vertical cluster possibly corresponding at surface to the Predjama high angle transpressional fault (PRJ) [64,91,6] seems to be linked at depth to ST, forming a SW-verging positive transpressional structure. A similar arrangement is also visible in section 2, where Predjama Fault and Susans-Tricesimo Th. interact at about 10 km depth. Note that the strongest event (May the 6th, Ml 6.4) affected the ST (earthquake n. 2 in Fig. 8, section 2), while the Ml 4.5 foreshock is located on the Predjama structure (earthquake n. 1 in Fig. 8, section 1). Therefore, the activation of the Predjama high angle fault during the earliest 1976 sequence can be hypothesized, and the possibility that its activation could have triggered the ST source, responsible of the mainshock of May 1976, must be taken into account. We rule out the activation of the Buia source (as proposed by [33]) because BU is characterized by a very low angle dipping geometry (about 20°) in the first kilometers depth (Fig. 5 and Fig. 8, section 2).

Moving towards the NW (Fig. 8, sections 3 and 4), the basal seismic level still corresponds to the POZ at about 14-15 km depth (which represents the base of the seismogenic thickness), while in the northeastern inner sector seismicity is confined by the Idrija-Ampezzo Fault System (IAFS). Differently from the southeastern area (sections 1 and 2), on sections 3 and 4, ST gives rise to a steeper ramp (about 40-45° dip) and extends deep up to 12 km depth. Moreover, in sections 3 and 4 seismicity mainly concentrates on high-angle structures depicted by means of a clear high angle

alignment of earthquakes. In particular, a well-developed structure, corresponding at surface to the high angle transpressional Maniaglia Fault (MAN) ("Gemona del Friuli geological Sheet", [23]) interacts at about 12 km depth with the ST steep ramp.

On the base of the field data, we rule out the possibility that these high angle structures could represent Gemona-Kobarid (GK) and Musi-Verzegnis (MV) Thrusts, since they both are characterized at surface by a middle dipping angle (about 45° dip) (Gemona del Friuli Geological Sheet and out of text figure 1, [23]). If considering the orientation of the seriated sections with respect to the thrusts geometry, GK and MV would appear with an even lower dip-angle, much different from the about 70° dipping plane observed on sections.

Focusing on the September – December 1976 sequence, we observe that most of seismicity develops in the northwestern sector of the study area (see also Fig. 7B) and is preferably located on a set of high-angle (60-80° dipping) structures (Fig. 9, sections 3 and 4), often characterized by oblique focal mechanisms (events n. 15, 16, 18 in Table 2 and Fig. 9, section 4), thus revealing their transpressive kinematics. In particular, sections 3 and 4 (Fig. 9) show the about 70° NE dipping alignment, probably representing the deep expression of the high-angle Maniaglia Fault (MAN). The location of the mainshock of September (Ml 6.1, event n. 13 in Table 2) suggests the activation of the NE deep portion of ST, which here extends deep up to 12 km and likely interacts at depth with the Maniaglia Fault. The remarkable seismic activity at the interaction depth between ST and MAN is already evident from the May-August 76 earthquakes distribution (Fig. 8, section 4). In this sector, also the Idrija-Ampezzo Fault System (IAFS) seems to be involved, acting as the northern backstop of seismicity.

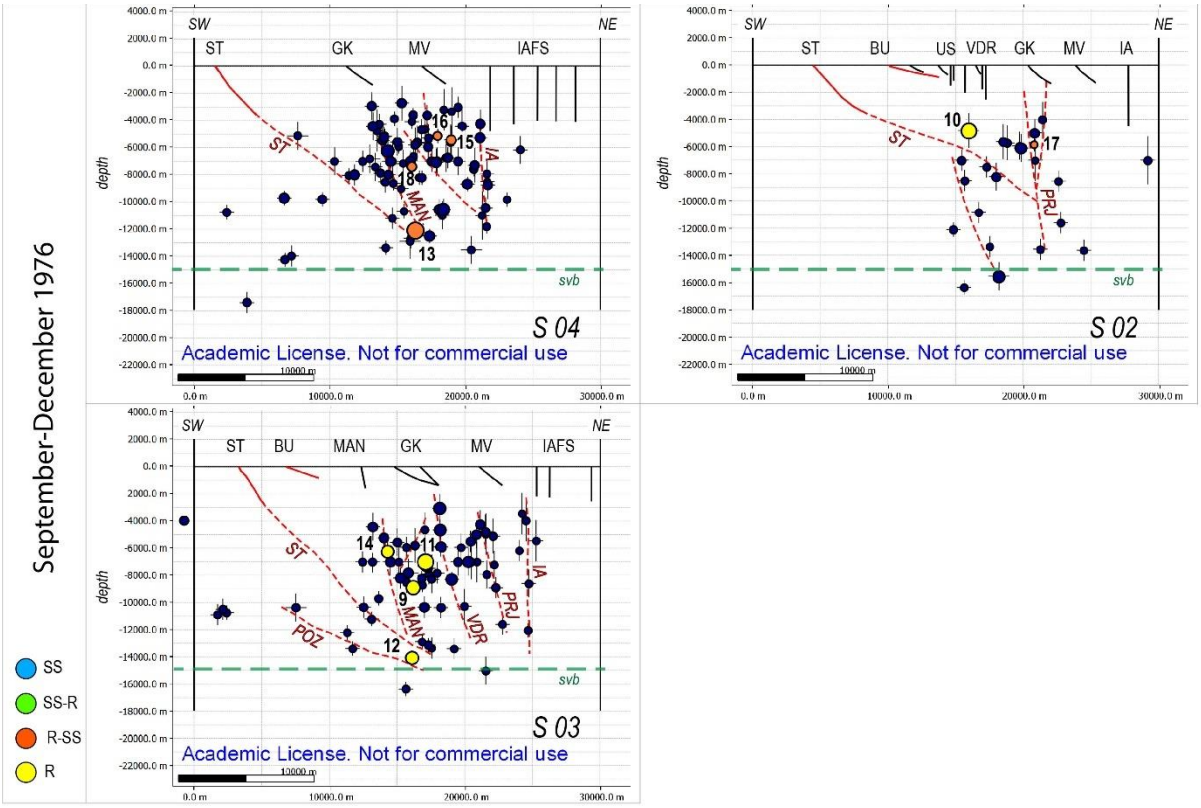

Figure 9. September - December 1976 Ml ≥ 2.5 seismicity plotted on the seriated sections ~~01~~, 02, 03, 04 (see traces in Fig. 6) together with the active faults surfaces reconstructed in this study (red thrusts) and tectonic structures known from the literature (black faults, [23]). The symbols size is proportional to the magnitude value (Ml), the number of the events refers to Table 2, while the color refers to the kinematics as shown in the legend. The vertical and horizontal bars for each event represent the vertical (Z) and horizontal (H) error localization, respectively. The red dashed lines refer to the interpretations of the activated structures, recognized on each section. The green dashed line represents the base of the seismogenic volume (svb). Faults acronyms: BFC: Borgo Faris – Cividale Fault-System; BU: Buia Thrust; GK: Gemona-Kobarid Th.; IAFS: Idrija-Ampezzo Ft. System; MV: Musi-Verzegnis Th.; PRJ: Predjama Ft.; ST: Susans-Tricesimo Th.; VDR: Vedronza Fault; US: Useunt Ft.

Concerning the southeastern sector (Fig. 9, section 2), seismicity is very ~~poor;~~ in analogy with the May-August distribution, we suppose that the earthquakes are bordered towards the NE by the high-angle Predjama Fault (PRJ). The reactivation of ST can be assessed from event n. 10 (Table 2).

During January – December 1977 seismicity decreased considerably, and the strongest event (n. 19 in Table 2) is located at the similar depth to the mainshock of September the 15th, but the scarcity of recorded earthquakes prevents any attribution to possible tectonic features.

Based on these results, it is worth to remark that a complex geometry characterizes ST structure spanning from the SE to the NW. Particularly, in sections 1 and 2 ST reaches about 10 km depth, by means of an about 30-35° dipping ramp, while in sections 3 and 4 it shows a steeper ramp (about 40-45° dipping) and reaches increasingly higher depths (up to 12 km) (Fig. 8), suggesting that ST surface is deformed rather than planar.

4.2.2. 1978-2019 seismicity

The collected and filtered 1978-2019-time interval seismicity of the study area (blue rectangle in Fig. 10) contains 2726 earthquakes with Md values spanning from 1 to 4.9. The frequency-depth graph (Fig. 10), in terms of number of events per 1 km depth class, shows that the 90 % of earthquakes is located in the first 15 km depth. Moreover, an abrupt increase of seismicity is evident at 7 km depth. If considering the magnitude Md of the events, the total released energy per depth class graph shows that most of the energy is released between 6 and 16 km depth since only few Md > 3.5 are registered in the first 5 km.

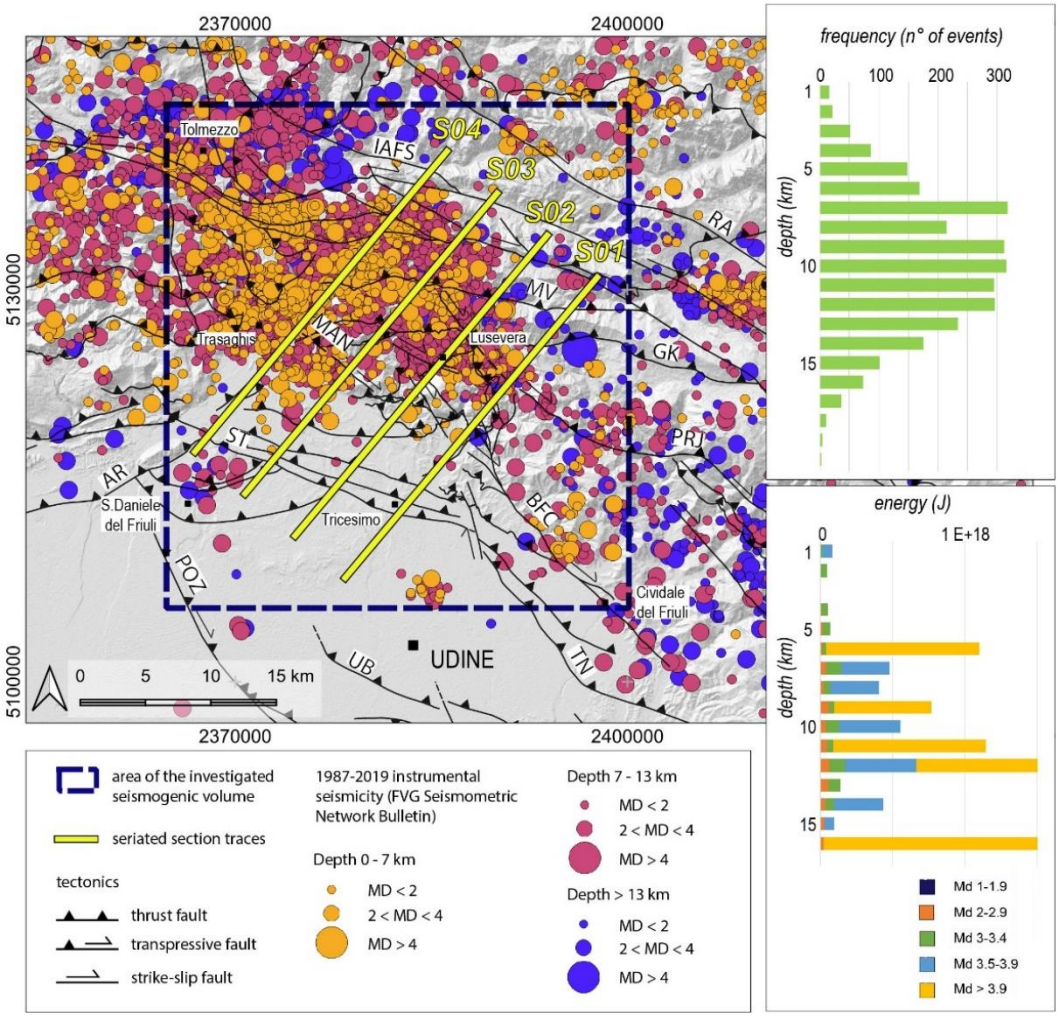

Figure 10. Map and depth 1978-2019 seismicity distribution of eastern Friuli – western Slovenia. The events are classified per depth and magnitude classes. Hypocentral frequency histograms of 1978-2019 seismicity are in terms of number of events per depth class and in terms of cumulated energy, differentiated per magnitude values, per depth classes.

In order to investigate the geometry of the seismogenic thickness, the collected events were classified in three macro-depth classes (0 – 7 km; 7 – 13 km and depth > 13 km) and the map distribution of each depth class was analyzed (Fig. 11).

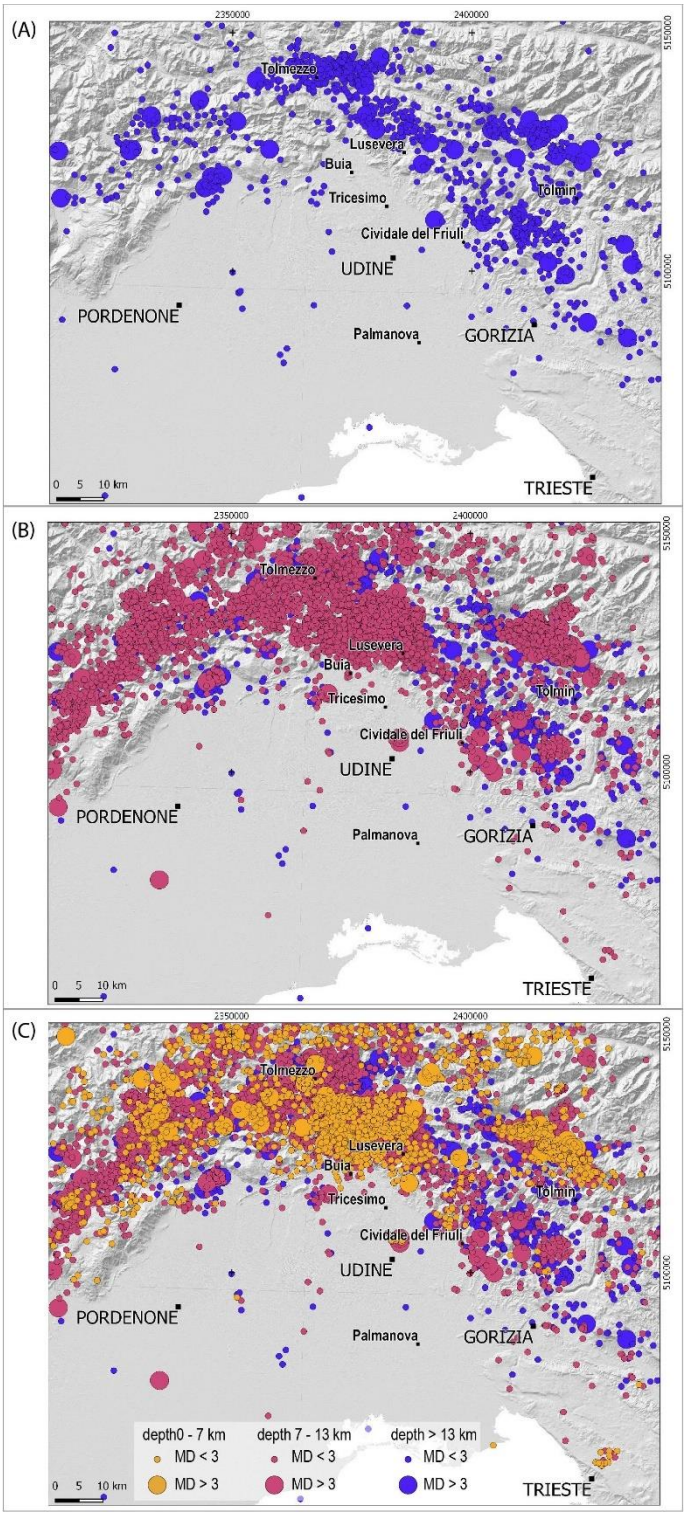

Figure 11. Map distribution of the 1978-2019 events at different depths. (A) Earthquakes with depth > 13 km; (B) earthquakes with depth > 7 km; (C) earthquakes with depth > 0 km.

Starting from the deeper events, the map of Fig. 11A highlights the main structural elements, testifying that this area represents the junction zone between the western NE-SW trending front in the western Carnic Prealps and the NW-SE trending eastern front

for the Julian Prealps and central Friuli area. Particularly, focusing on the study area, the events located at depth greater than 13 km (Fig. 11A) depict a clear NW-SE alignment, from Tolmezzo to Gorizia. Moving up at shallower depth (Fig. 11B), the earthquakes between 7 and 13 km depth affect a wider area, expanding South of the Tolmezzo – Gorizia alignment. The southern border of 7 – 13 km seismicity is characterized by a WNW-ESE orientation in the central portion of the study area while SE of Tricesimo, seismicity is distributed along a NW-SE alignment matching the deeper (>13 km) seismicity distribution. Any major details can be added from the shallowest seismicity distribution analysis (0 - 7 km, Fig. 11C), which is widely distributed. Regarding surficial seismicity, it is worth to remember that only the 17 % of earthquakes is located in the first 6 km depth with one event exceeding Md > 3.5. Anyhow, the three maps of Fig. 11 well highlight two active regions: the arcuate mostly compressive pre-alpine and alpine portion of Southalpine Chain and the strike-slip domain of western Slovenia, related by a transpressional sector.

In good agreement with the 76-77 sequence distribution previously analyzed, the 1978–2019-time interval earthquakes plotted on the seriated sections (Fig. 12) show that spanning from the SE to the NW seismicity affects the entire seismogenic thickness, which extends deep up to 15 km, progressively involving a wider crustal volume. In this context, it is worth to remark that the post 1977 seismicity refers to an interseismic, therefore the earthquakes distribution well highlights the active seismogenic crustal volume as a whole, but the individual structures inside of it are not clearly recognizable.

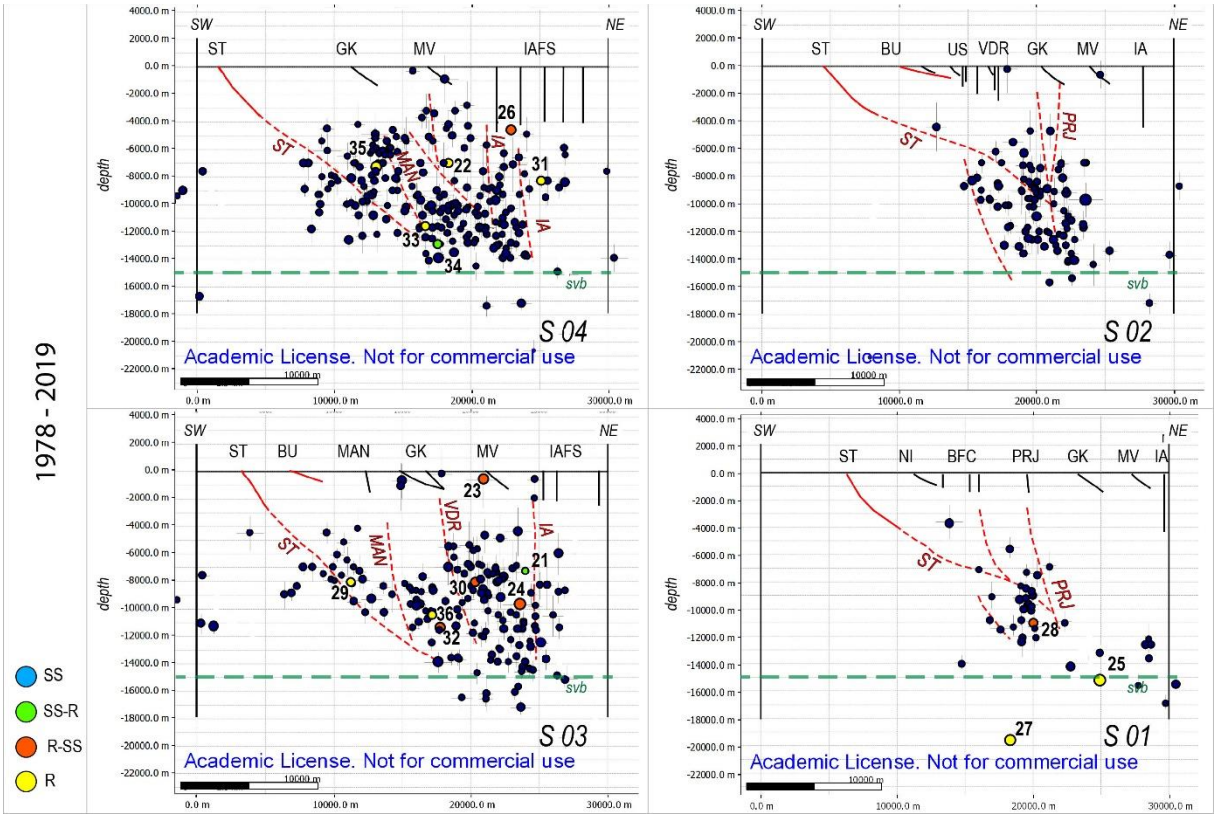

Figure 12. Seriated sections 01, 02, 03 and 04 (see Fig. 6 for section traces). The filtered 1978-2019 Md ≥ 2 seismicity was plotted together with the active faults surfaces reconstructed in this study (red thrusts) and tectonic structures known from the literature (black faults, [23]). The symbols size is proportional to the magnitude value (Md), the number of the events refers to Table 3, while the color refers to the kinematics as shown in the legend. The vertical and horizontal bars for each event represent the vertical (Z) and horizontal (H) error localization, respectively. The red dashed lines refer to the interpretations of the activated structures, recognized on each section. The green dashed line represents the base of the seismogenic volume (svb). Faults acronyms: BFC: Borgo Faris – Cividale Fault-System; BU: Buia Thrust; GK: Gemona-Kobarid Th.; IAFS: Idrija-Ampezzo Ft. System; MV: Musi-Verzegnis Th.; PRJ: Predjama Ft.; ST: Susans-Tricesimo Th.; VDR: Vedronza Fault; US: Useunt Ft.

Table 3. Collection of analyzed focal mechanisms of the 1978-2019 time interval seismicity. FT refers to the fault type classification by [82], as indicated in [7].

	EVENT PARAMETERS [8]			**Preferred Focal Mechanism** [7]		
ID	**DATE**	**TIME**	**DEPTH [km]**	**MD**	**FT**	**REF**
21	02/04/1978	18:23	7.3	2.4	SS-R	[81]
22	03/04/1978	14:34	7	3.1	R	[81]
23	02/12/1978	04:05	0.6	3.5	R-SS	[81]
24	30/08/1981	23:30	9.7	3.9	R-SS	[3]
25	10/02/1983	22:30	15.1	4.2	R	[36]
26	20/12/1983	08:26	4.6	3.4	R-SS	[36]
27	05/10/1991	05:14	19.5	3.8	R	[36]
28	05/10/1991	14:56	10.9	3.1	R-SS	[3]
29	25/07/1995	11:53	8.1	3	R	[36]
30	22/12/1996	03:49	8.1	3.2	R-SS	[36]
31	09/12/1997	01:36	8.3	3.1	R	[36]
32	06/07/2002	08:30	11.4	3.5	R-SS	[36]
33	11/08/2006	01:35	11.6	3.1	R	[36]
34	23/03/2017	13:11	12.9	3.1	SS-R	[36]
35	09/05/2018	21:48	7.3	3.7	R	[92]
36	10/11/2018	07:59	10.5	3	R	[92]

The southeastern portion of the study area is characterized by a tighter seismogenic volume: in sections 1 and 2 (Fig. 12) the earthquake distribution is limited towards the NE by the high-angle Predjama Fault and by a frontal medium-high angle plane towards the SW. The latter correlates with the deep steep ramp which develops at the footwall of ST, as already identified from the 1976-1977 sequence distribution (Figs. 8 and 9, sections 1 and 2).

In the northwestern portion of the study area, sections 3 and 4 (Fig. 12) show that seismicity abruptly decreases towards the NE in correspondence of the Idrija-Ampezzo strike-slip Fault System (IAFS), while regarding the first 20 km length of the sections, the plotted earthquakes are limited at depth by means of an about 40° NE-dipping plane, probably correlating to the ST. Contrary to the 1976 seismic sequence, only scarce seismic activity can be related to POZ (Fig. 12).

4. Discussion

The seismicity of central-eastern Friuli region was investigated through the hypocentral distribution analysis of the earthquakes registered in the last 50 years starting from the two seismic sequences occurred in May and September 1976. The earthquakes distribution analysis was also compared both with the deep geometry of the tectonic structures obtained from the interpretation of ENI industrial seismic lines in 3D Move (STTS in this paper and POZ in [27] and with the surface geological data available from the literature [66,69,23]. Both subsurface and surficial data highlight significant structural complexities derived from the polyphase deformational evolution which affected the study area. The results obtained in this work allowed us to better characterize the seismotectonic model of central-eastern Friuli region and also to formulate new hypotheses regarding the seismogenic sources of the recent strongest earthquakes.

The eastern Southalpine area reveals an articulated geological evolution, within which the inherited tectonic structures have always played a fundamental role, strongly

conditioning the geometry and the kinematics of the structural elements activated during the successive deformative stages. At present, the seismotectonic framework of the study area is characterized by different deformational domains: towards the East, in western Slovenia area, stress is accommodated through pure strike-slip kinematics by NW-SE (Dinaric trending) fault systems [6], while the Venetian and Carnic prealpine regions are characterized by a dominantly dip-slip motion accommodated by the ENE-WSW striking eastern Southalpine fronts [93]. At the transition between the two structural domains, the alpine and prealpine Julian regions define a compressional domain with a strong oblique component [4,26].

Focusing on the earthquakes, the seismicity of the eastern domain is mainly referable to the dextral strike-slip fault systems, as testified by the most recent events of Bovec (1998, Mw 5.6) and Tolmin (2004, Mw 5.2) associated to the Ravne strike-slip fault [29]. Differently, the genesis of the destructive historical earthquake of March the 26th 1511 is more debated, but many Authors refer it to the strike-slip fault systems of western Slovenia: the CFTMed05 Catalogue [39] suggests the Predjama Fault as seismogenic source, [40,34] indicate the Idrija Fault, while [26] propose the activation of the Borgo Faris-Cividale Fault. Moving to the western domain, in central Friuli area the widespread presence of many high-angle to subvertical fault segments, often connected by structural bend and step-over zones [23,94], testifies the active north-westward propagation of the dextral strike-slip fault systems. In this sector, slip is accommodated through the partitioning between strike-slip fault segments and the inherited reverse planes from the Paleogene Dinaric orogeny, which were affected by deformation during the Neoalpine polyphase tectonics (Pliocene – Quaternary phase in [19]; Messinian – Pliocene phase in [12,15,20,16]). At surface, the presence of dome and basin structures is documented all over the central Friuli region and is related to the superimposition of the Neoalpine (σ1=NW-SE to NNW-SSE) tectonics over the Dinaric (σ1=NE-SW) compression. In the central Friuli area, polydeformed structures have already been documented and mapped by [95], who assigned a tectonic origin to the Arzino, Bernadia and Natisone "Ellipsoid". [96,97,23] described the SE-verging macrofold of Covria Mt., on the right bank of the Tagliamento river. [98,99] analyzed the polyphase structural framework of the Bernadia Mts. and [100], through a detailed structural analysis of the area located South of the Gemona-Kobarid Thrust, confirmed the relationship between dinaric and neoalpine tectonics as already suggested by [88].

Moreover, the geological field data presented by [66,23] testify that in the northern portion of the Friuli Plain the sub-surfacing pre-Quaternary succession is characterized by dome and basin structuring and is generally tilted towards the North. Particularly, while in the whole eastern sector and Buia area the pre-Quaternary terms consist of Eocene turbiditic units affected by ENE-WSW trending folding, in the northwestern portion, among the Susans Hill, Osoppo and Trasaghis relieves border, a reduced succession of Southalpine Molasse outcrops [23].

The hypocentral distribution analysis of the 1976 seismic sequences conducted in this study allowed the 3D-reconstruction of the seismogenic volume of central Friuli region, which corresponds to the first 15 km depth, in good agreement with [101]. In detail, the elaboration realized through the 3D Move Software highlighted the folded geometry of the Susans-Tricesimo Thrust System with an about 20-30° N-dipping axial plane (Fig. 13), likely representing the result of the superimposition of the Pliocene tectonic evolution over the Dinaric compressional phase. The reconstructed deformed surface defines two distinct planes which are probably subjected to different shortening rates: the southeastern surface, characterized by a mean dipping geometry N33°/30°, is connected at about 10 km depth with the Predjama high angle transpressional fault. Differently, the north-western segment plane shows a mean N30°/40° dipping geometry and reaches higher depths interacting at about 12 km with the Maniaglia fault. On the first surface (ST-SW) lies the mainshock of May 1976 (Ml 6.4) (Fig. 8, section 1-2 and Fig. 13), while the strongest event

of September 1976 (Ml 6.1) is located on the deepest portion of ST-NW segment, right at the interaction depth with the Maniaglia Fault (Fig. 9 sez. 3-4 and Fig. 13).

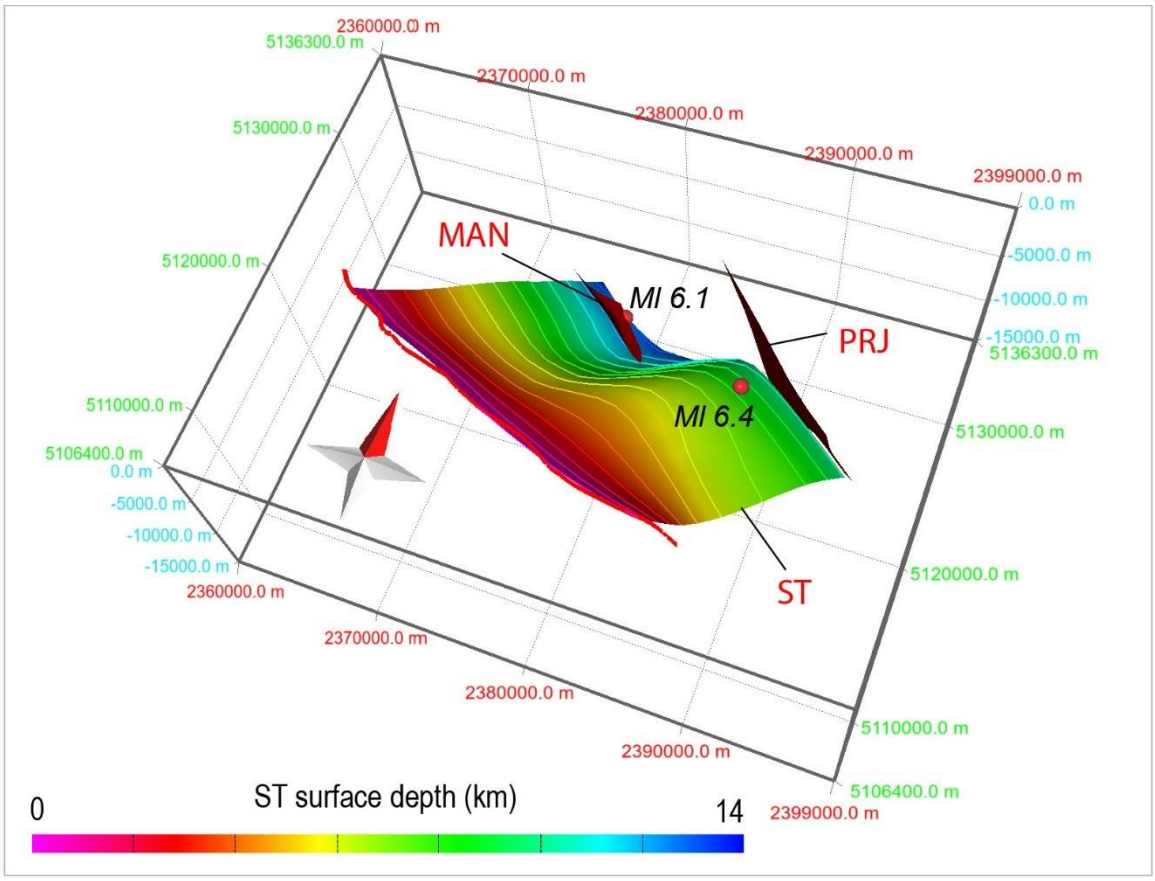

Figure 13. 3D deep surface of Susans-Tricesimo Thrust (ST), Maniaglia Fault (MAN) and Predjama Fault (PRJ), reconstructed through the hypocentral distribution analysis. The red circles represent the hypocenters of the strongest events of May (Ml 6.4) and September (Ml 6.1), respectively.

On the basis of these statements, important implications in terms of seismogenesis arise: as a consequence of the structural complexities characterizing the deep geometry of the Susans-Tricesimo Thrust, combined with the articulated strain regime of the area, it is likely that the southeastern and northwestern portions of ST define two distinct seismogenic segments. Particularly, the depicted seismotectonic framework suggests that the Ml 6.4 mainshock of May 1976 ruptured the solely southeastern portion (ST-SE) and was likely triggered by the Predjama Fault, which was responsible of the Ml 4.5 foreshock. Following the strongest event, most of the aftershocks migrated towards the NW affecting the area of higher structural complexity. Later, the Ml 6.1 mainshock of 15th of September ruptured the deepest portion of the ST-NW seismogenic segment, at the depth of interaction with the Maniaglia Fault, which was also activated during the second part of the sequence (Fig. 14).

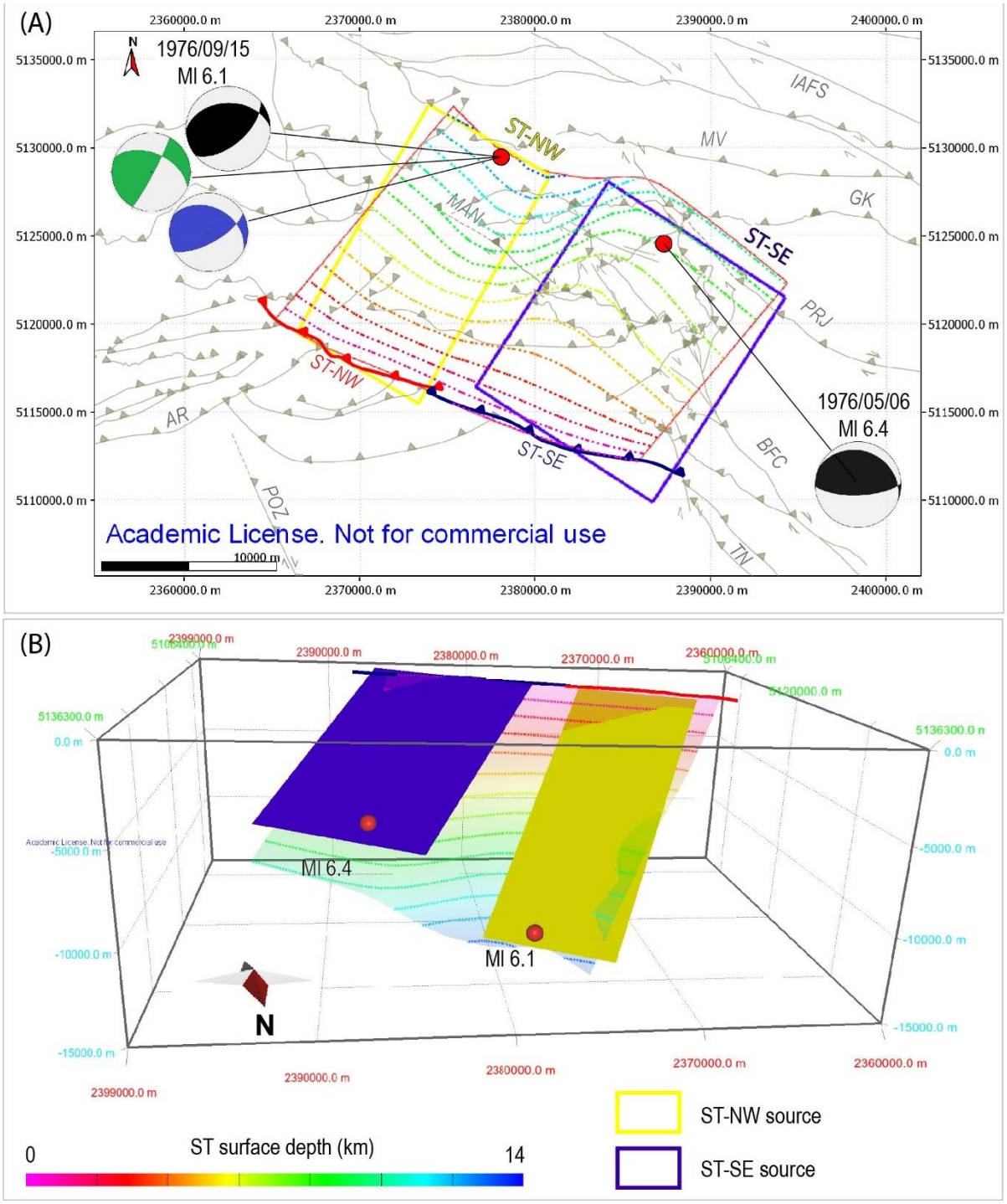

Figure 14. Schematic representation of the seismotectonic model elaborated for the study area. (A) Map view where the colored isolines refer to the ST surface reconstructed from the seismicity distribution analysis; the yellow and blue box represent the seismogenic sources associated to the ST-NW and ST-SE segments. Red circles represent the strongest earthquakes of May (Ml 6.4) and September (Ml 6.1). (B) 3D-view of the seismotectonic model. Black focal mechanisms from [81], blue from [87] and green from [88].

If considering the presence of a medium earthquake during the hours immediately before the mainshock of September the 15th (event n. 11 in Table 2), located on the Maniaglia Fault alignment (Fig. 9, section 3), it is likely that the Maniaglia Fault triggered the Susans-Tricesimo northwestern segment, similarly to the interplay likely occurred during the May sequence between Predjama Fault and southeastern Susans-Tricesimo segment. In this regard, it is worth to remark that [87] proposed a focal mechanism for the

mainshock of September which shows the activation of a 30° dipping NW-SE striking plane with a significant dextral component, in good agreement with the focal mechanism solution proposed by [88]. Both interpretations, which only slightly differ from the 38° N-dipping geometry of [81], ~~perfectly~~ match ~~and strongly support~~ our hypothesis regarding the activation of the ST-NW segment as the source of the Ml 6.1 September earthquake.

On the basis of the 3D seismotectonic model reconstructed, the seismotectonic parameters of the identified seismogenic segments are presented in Table 4. Particularly, starting from the length (SRL) and the area (RA) of each source, the maximum expected values were calculated through the [102] empirical relationships considering both thrust-fault (TH) and all type (ALL) kinematics. The estimated Mmax values for both ST-SE and ST-SW well represent the seismogenic potential of the strongest events of the 1976 Friuli sequences.

Table 4. Seismotectonic parameters of ST-SE and ST-NW seismogenic source segments [102].

SEISMOGENIC SOURCE	L [km]	H [km]	DIP STRIKE [°]	DIP [°]	W [km]	RA [km²]	Mmax (SRL)-TH	Mmax (SRL)-ALL	Mmax (RA)-TH	Mmax (RA)-ALL
ST-SE	12	10	33	30	20	240	6.3	6.3	6.5	6.4
ST-NW	8	12	30	40	18.7	149.3	6.1	6.1	6.3	6.2

5. Conclusions

By integrating 3D structural setting reconstructed from ENI seismic lines interpretation (up to 5 km depth), the seismogenic upper crustal volume investigated through the hypocentral seismicity distribution analysis (up to 15 km depth) and the surficial structural setting of the central Friuli area, we reconstructed the present seismotectonic model of the southern Julian Prealps and northern Friuli Plain. The kinematic model features that:

- the seismogenesis of the area is strongly defined by the structural inheritance, especially in terms of structural complexities representing the product of the combined effect of the Paleogene Dinaric orogeny and the late Miocene – Pliocene Neoalpine compression;
- because of its deep structural complexity, the polyphasic Susans-Tricesimo masterfault is likely segmented in two distinct seismogenic sources (ST-SE and ST-NW);
- the NW-ward propagating dextral transpressive fault systems of western Slovenia are affecting the inherited thrusts, and the Dinaric trending transpressive fault segments strongly control the strain accommodation in the central Friuli area, as already remarked by [26,25]. In this context, the possibility that September 15th 1976 mainshock was induced by a transpressive source, corresponding at surface with the Maniaglia fault, is not excluded. While regarding the mainshock of May 6th 1976, the southeastern segment of ST was likely triggered by the Predjama Fault;
- the activation of Buia Thrust during the strongest events of 1976 sequences is ruled out and the involvement of the Gemona-Kobarid and Musi-Verzegnis thrusts is reduced.This section is not mandatory but can be added to the manuscript if the discussion is unusually long or complex.

Author Contributions: Conceptualization, Giulia Patricelli and Maria Eliana Poli; Data curation, Maria Eliana Poli; Funding acquisition, Maria Eliana Poli; Investigation, Giulia Patricelli; Methodology, Giulia Patricelli; Supervision, Maria Eliana Poli; Writing – original draft, Giulia Patricelli; Writing – review & editing, Maria Eliana Poli.

Funding: This research was realized in the framework of the Environmental Life Science PhD Course XXXIII cycle managed by the University of Trieste and the University of Udine. The study was supported by the *Accordo Attuativo di collaborazione per approfondire la conoscenza delle faglie attive nel territorio regionale* signed by Regione Autonoma Friuli Venezia Giulia – Direzione centrale difesa dell'ambiente, energia e sviluppo sostenibile, the Dipartimento di Matematica e Geoscienze dell'Università degli Studi di Trieste, il Dipartimento di Scienze AgroAlimentari, Ambientali e Animali dell'Università di Udine and the Istituto Nazionale di Oceanografia e Geofisica Sperimentale.

Data Availability Statement:
The interpreted seismic lines are property data of ENI.
Focal mechanisms are from the Catalogue of earthquakes of southern Alps and surroundings area from 1928 to 2019, available online at https://zenodo.org/record/4660412#.Yjn_WurMLIU.
Seismological data of the 1978-2019 earthquakes are from the OGS-CRS Friuli Venezia Giulia Seismometric Network Bulletin, available online at http://www.crs.inogs.it/bollettino/RSFVG/RSFVG.en.html.

Acknowledgments: We acknowledge ENI for the consultation and supply of seismic data. We thank Petroleum Expert Ltd for the availability of the 3D-Move Software to the University of Udine. We are grateful to A. Saraò, A. Rebez and G. Renner for the critical discussion during the manuscript writing. Many thanks to A. Zanferrari for his constructive suggestions and to L. Ronchiadin for his contribution to seismic lines interpretation.

Conflicts of Interest: The authors declare no conflict of interest.

References

1. Serpelloni, E.; Vannucci, G.; Anderlini, L.; Bennet, R.A. Kinematics, seismotectonics and seismic potential of the eastern sector of the European Alps from GPS and seismic deformation data. *Tectonophysics* **2016,** *688*, 157-181. DOI https://doi.org/10.1016/j.tecto.2016.09.026.
2. Galadini, F.; Poli, M.E.; Zanferrari. A. Seismogenic sources potentially responsible for earthquakes with M≥6 in the eastern Southern Alps (Thiene-Udine sector, NE Italy). *Geophys. J. Int.* **2005,** *161*, 739-762. DOI 10.1111/j.1365-246X.2005.02571.x.
3. Poli, M.E.; Renner, G. Normal focal mechanisms in the Julian Alps and Prealps seismotectonic implications for the Italian-Slovenian border region. *Boll. Geof. Teor. Appl*. **2004**, *45*, 51-69.
4. Vrabec, M.; Fodor, L. Late Cenozoic tectonics of Slovenia: structural styles at the Northeastern corner of the Adriatic microplate. In: *The Adria microplate: GPS geodesy, tectonics and hazards*. Springer, Dordrecht 2006, pp. 151-168.
5. Moulin, A.; Benedetti, L.; Rizza, M.; Rupnik, P.J.; Gosar, A.; Bourlès D.; Keddadouche, K.; Aumaitre, G.; Arnold, M.; Gçuillou, V.; Titz, J.-F. The Dinaric fault system: large-scale structure, rates of slip, and Plio-Pleistocene evolution of the transpressive northeastern boundary of the Adria microplate. *Tectonics* **2016**, *35*. DOI 10.1002/2016TC004188.
6. Atanackov, J.; Jamšek Rupnik. P.; Jež, J.; Celarc, B.; Novak, M.; Milanič, B.; Markelj, A.; Bavec, M.; Kastelic, V. Database of Active Faults in Slovenia: Compiling a New Active Fault Database at the Junction Between the Alps, the Dinarides and the Pannonian Basin Tectonic Domains. *Front. Earth Sci.* **2021**, *9*, 151. doi: 10.3389/feart.2021.604388.
7. Saraò, A.; Sugan, M.; Bressan, G.; Renner, G.; and Restivo, A. A focal mechanism catalogue of earthquakes that occurred in the southeastern Alps and surrounding areas from 1928–2019. *Earth System Science Data* **2021**, *13*, 2245-2258. https://doi.org/10.5194/essd-13-2245-2021.
8. OGS-CRS: Friuli Venezia Giulia Seismometric Network Bulletin. http://www.crs.inogs.it/bollettino/RSFVG/RSFVG.en.html (Accessed December 2021).
9. Roeder, D. South-Alpine thrusting and trans-Alpine convergence. In: *Alpine Tectonics*. Coward, M.P., Dietrich, D., Park, R.G. Eds., Geol. Soc. London Spec. Publ. 1989, *45*, 211-227.
10. Castellarin, A.; Nicolich, R.; Fantoni, R.; Cantelli, L.; Sella, M.; Selli, L. Structure of the lithosphere beneath the Eastern Alps (southern sector of the TRANSALP transect). *Tectonophysics* **2006**, *414*, 259-282. DOI 10.1016/j.tecto.2005.10.013.
11. Doglioni, C.; Bosellini, A. Eoalpine and mesoalpine tectonics in the Southern Alps. *Geol. Rundsch.* **1987**, *76*, 735-754.
12. Castellarin, A.; Cantelli, L.; Fesce, A.M.; Mercier, J.L.; Picotti, V.; Pini, G.A.; Prosser, G.; Selli, L. Alpine compressional tectonics in the Southern Alps. Relationships with the N-Apennines. *Ann. Tectonicae* **1992**, *6*, 62-94.
13. Fantoni, R.; Catellani, D.; Merlini, S.; Rogledi, S.; Venturini, S. La registrazione degli eventi deformativi cenozoici nell'avampaese Veneto-Friulano. *Mem. Soc. Geol. It.* **2002**, *57*, 301-313.
14. Monegato, G.; Stefani, C.; Zattin, M. From present rivers to old terrigenous sediments: the evolution of the drainage system in the eastern Southern Alps. *Terra Nova* **2010**, *22(3)*, 218-226. https://doi.org/10.1111/j.1365-3121.2010.00937.x
15. Castellarin, A.; Cantelli L. Neo-Alpine evolution of the Southern Eastern Alps. J. *Geodyn.* **2000**, *30*, 251-274.
16. Caputo, R.; Poli, M.E.; Zanferrari, A. Neogene-Quaternary stratigraphy of the eastern Southern Alps, NE Italy. *J. Struct. Geol.* **2010**, *32*, 1009-1027. DOI 10.1016/j.jsg.2010.06.004.
17. Toscani, G.; Marchesini, A.; Barbieri, C.; Di Giulio, A.; Fantoni, R.; Mancin, N; Zanferrari, A. The Friulian-Venetian Basin I: architecture and sediment flux into a shared foreland basin. *Ital. J. Geosci.* **2016**, *135 (3)*, 444-459. DOI 10.3301/IJG.2015.35.
18. Massari, F.; Grandesso, P.; Stefani, C.; Jobstraibizer, PG. A small polyhistory basin evolving in a context of oblique convergence: the Venetian basin (Chattian to Recent, Southern Alps, Italy). In: *Foreland Basins.* Allen, P.A.; Homewood, P. Eds., Blackwell Scientific Oxford 1986, 141-168.
19. Venturini, C. Cinematica neogenico-quaternaria del Sudalpino orientale (settore friulano), *Studi Geol. Cam*. **1990**, spec. vol. 1990, 109-116.
20. Monegato, G. Le successioni conglomeratiche messiniano-pleistoceniche nel bacino del fiume Tagliamento. Ph.D. thesis. University of Udine, Udine **2006.**
21. Caputo, R.; Poli, M.E.; Zanferrari, A. Neogene-Quaternary Twist tectonics in the eastern southern Alps, Italy. *Memorie di Scienze Geologiche* **2003**, *54*, 155-158.
22. Caputo, R. The polyphase tectonics of eastern Dolomites, Italy. *Memorie di Science Geologiche* **1996**, *48*, 93-106.
23. Zanferrari, A.; Masetti, D.; Monegato, G.; Poli M.E. Geological map and explanatory notes of the Geological Map of Italy at the scale 1:50.000: sheet 049 "Gemona del Friuli". ISPRA – Servizio Geologico d'Italia – Regione Autonoma Friuli Venezia Giulia **2013**, 262 pp. www.isprambiente.gov.it/Media/carg/friuli.html.
24. Márton, E.; Cosovic, V.; Drobne, K.; Moro, A. Palaeomagnetic evidence for Tertiary counterclockwise rotation of Adria. *Tectonophysics* **2003**, *377*, 143-156.
25. Poli, M.E.; Zanferrari, A. The seismogenic sources of the 1976 Friuli earthquakes: a new seismotectonic model for the Friuli area. *Boll. Geof. Teor. Appl.* **2018**, *59*, 463-480. DOI 10.4430/bgta0209.
26. Falcucci, E.; Poli, M.E.; Galadini, F.; Scardia, G.; Paiero, G.; Zanferrari, A. First evidence of active transpressive surface faulting at the front of the Eastern Southern Alps, northeastern Italy. Insight on the 1511 earthquake seismotectonics. *Solid Earth* **2018**, *9*, 911-922. DOI https://doi.org/10.5194/se-9-911-2018.

27. Patricelli, G.; Poli, M. E. Quaternary tectonic activity in the north-eastern Friuli Plain (NE Italy). *Boll. Geof. Teor. Appl.* **2020**, *61(3)*, 309-332. DOI 10.4430/bgta0319.
28. Poljak, M.; Živčić, M.; Zupančič, P. The seismotectonic characteristics of Slovenia. In: *Seismic Hazard of the Circum-Pannonian Region*, Birkhäuser, Basel. **2000**, pp. 37-55.
29. Kastelic, V.; Vrabec, M.; Cunningham, D.; Gosar, A. Neoalpine structural evolution and present day tectonic activity of the eastern Southern Alps: the case of the Raune fault, NW Slovenia. *J. Structural Geol.* **2008**, *30*, 963-965. DOI 10.1016/j.jsg.2008.03.009.
30. Moulin, A.; Benedetti, L.; Gosar, A.; Rupnik, P.J.; Rizza, M.; Bourlès, D.; Ritz, J. Determining the present-day kinematics of the Idrija fault (Slovenia) from aiborne LiDAR topography. *Tectonophysics* **2014**, *628*, 188-205. DOI http://dx.doi.org/10.1016/j.tecto.2014.04.043.
31. Bechtold, M.; Battaglia, M.; Tanner, D.C.; Zuliani, D. Constraints on the active tectonics of the Friuli/NW Slovenia area from CGPS measurements and three-dimensional kinematic modeling. *J. Geophys. Res.* **2009**, *114(B3)*. DOI 10.1029/2008JB005638.
32. Devoti, R.; Esposito, A.; Pietrantonio, G.; Pisani, A.R; Riguzzi, F. Evidence of large scale deformation patterns from GPS data in the Italian subduction boundary. *Earth Planet. Sci. Lett.* **2011** *311*, 230-241. DOI 10.1016/j.epsl.2011.09.034.
33. Cheloni, D.; D'Agostino, N.; D'Anastasio, E.; Selvaggi, G. Reassessment of the source of the 1976 Friuli, NE Italy, earthquake sequence from the joint inversion of high-precision levelling and triangulation data. *Geophys. J. Int.* **2012**, *190*, 1279-1294. DOI 10.1111/j.1365-246X.2012.05561.x.
34. Grützner, C.; Aschenbrenner, S.; Rupnik, P.J.; Reicherter, K.; Saifelislam, N.; Včič, B.; Vrabec, M.; Welte, J.; Ustaszewski, K. Holocene surface rupturing earthquakes on the Dinaric Fault System, western Slovenia. *Solid Earth* **2021**, *12*, 2211-2234. https://doi.org/10.5194/se-12-2211-2021.
35. OGS-CRS: Friuli Venezia Giulia Seismometric Network. http://rts.crs.inogs.it/ [Accessed December 2021]
36. Bressan, G.; Barnaba, C.; Bragato, P.; Ponton, M.; Restivo, A. Revised seismotectonic model of NE Italy and W Slovenia based on focal mechanism inversion. *J. Seismol.* **2018**, 22(6), 1563-1578. https://doi.org/10.1007/s10950-018-9785-2.
37. Rovida, A.; Locati, M.; Camassi, R.; Lolli, B.; Gasperini P; Antonucci A. Catalogo Parametrico dei Terremoti Italiani (CPTI15), versione 4.0. Istituto Nazionale di Geofisica e Vulcanologia, **2022.** DOI https://doi.org/10.13127/CPTI/CPTI15.4.
38. Camassi, R.; Caracciolo, C.H.; Castelli, V.; Slejko, D. The 1511 Eastern Alps earthquakes: a critical update and comparison of existing macroseismic datasets. *J. Seismol.* **2011**, *15*, 191-213. DOI: 10.1007/s10950-010-9220-9.
39. Guidoboni, E.; Ferrari, G.; Tarabusi, G.; Sgattoni, G.; Comastri, A.; Mariotti, D.; Ciuccarelli, C.; Bianchi, M.G.; Valensise G. CFTI5Med, the new release of the catalogue of strong earthquakes in Italy and in the Mediterranean area. *Scientific Data* **2019**, *6(1)*, 1-15. doi: https://doi.org/10.1038/s41597-019-0091-9.
40. Fitzko, F.; Suhadolc, P.; Aoudia, A.; Panza, G.F. Constraints on the location and mechanism of the 1511 Western-Slovenia earthquake from active tectonics and modeling of macroseismic data. *Tectonophys*. **2005**, *404*, 77-90. doi: 10.1016/j.tecto.2005.05.003.
41. Ribaric, V. The Idrija earthquake of March 26, 1511. A reconstruction of some seismological parameters. *Tectonophys*. **1979**, *53*, 315-324.
42. Bavec, M.; Atanackov, J.; Celarc, B.; Hajdas, I.; Jamšek, R.; Jež, J.; Kastelic, V.; Milanič, B.; Novak, M.; Skaberne, G.; Žibret, G. Evidence of Idrija fault seismogenic activity during the Late Holocene including the 1511 Mm 6.8 earthquake. In: *Proceedings: 4th International INQUA Meeting on Paleoseismology, Active Tectonics and Archeoseismology*. Grützner & Reicherter Geosolutions Aachen **2013**, 23-26.
43. Slejko, D. What science remains of the 1976 Friuli earthquake? *Boll. Geof. Teor. Appl.* **2018**, *59*, 327-350. doi: 10.4430/bgta0224.
44. Steinhauser, P.; Lenhardt, W. Interpretation of crustal deformations in the Friuli area for the earthquake of 1976. *Gerlands Beitr. Geophys*. **1986**, *95*, 459-467.
45. Talamo, R.; Pampaloni, M.; Grassi, S. Risultati delle misure di livellazione di alta precisione eseguite dall'Istituto Geografico Militare nelle zone del Friuli interessate dalle recenti attività sismiche. *Boll. Geod. Sci. Aff.* **1978**, *1*, 6-75.
46. Regione Autonoma Friuli Venezia Giulia. Misure geodetiche per la misura delle deformazioni del suolo nella zona a maggiore sismicità della Regione Friuli Venezia Giulia. Università di Udine, Rapporto inedito, **2005**, pp 65.
47. Amato, A.; Barnaba, P.F.; Finetti, I.; Groppi, G.; Martins, B.; Muzzin, A. Geodynamic outline and seismicity of Friuli Venetia Julia region. *Boll. Geof. Teor. Appl.* **1976**, *18*, 217-256.
48. Aoudia, A.; Saraò, A.; Bukchin, B.; Suhadolc, P. The 1976 Friuli (NE Italy) thrust faulting earthquake: a reappraisal 23 years later. *Geophys. Res. Lett.* **2000,** *27*, 573-576.
49. Poli, M.E.; Peruzza, L.; Rebez, A.; Renner, G.; Slejko, D.; Zanferrari, A. New seismotectonic evidence from the analysis of the 1976-1977 and 1977-1999 seismicity in Friuli (NE Italy). *Boll. Geof. Teor. Appl.* **2002**, *43*, 53-78.
50. Pondrelli, S.; Ekström, G.; Morelli, A. Seismotectonic re-evaluation of the 1976 Friuli, Italy, seismic sequence. *J. Seismol.* **2001**, *5*, 73-83.
51. Bernardis, G.; Poli, M.E.; Snidarcig, A.; Zanferrari, A. Seismotectonic and macroseismic characteristics of the earthquake of Bovec (NW Slovenia: April 12, 1998). *Boll. Geof. Teor. Appl*. **2000**, *41*, 133-148.
52. Bajc, J.; Aoudia, A.; Saraò, A.; Suhadolc, P. The 1998 Bovec-Krn mountain (Slovenia) earthquake sequence. *Geophys. Res. Lett.* **2001,** *28 (9)*, 1839-1842.
53. Zupancîč, P.; Cecić, I.; Gosar, A.; Placer, L.; Poljak, M.; Živčić, M. The earthquake of 12 April 1998 in the Krn Mountains (Upper Soča valley, Slovenia) and its seismotectonic charcteristics. *Geologija* **2001**, *44*, 169-192.

54. Živčić, M.; Krn-2004 team. The Krn mountains (Slovenia) Mw 5.2 earthquake: data acquisition and preliminary results. *Geoph. Res. Abstr.* **2006**, *8*, 06439.
55. Mancin, N.; Barbieri, C.; Di Giulio, A.; Fantoni, R.; Marchesini, A.; Toscani, G.; Zanferrari, A. The Friulian-Venetian Basin II: paleogeographic evolution and subsidence analysis from micropaleontological constraints. *Ital. J., Geosci.* **2016**. *135 (3),* 460-473, DOI 10.3301/IJG.2015.35.
56. Cousin, M. Les rapports Alpes-Dinarides. Les confines de l'Italie et de la Yugoslavie. *Soc. Géol. Nord* **1981**, *5 (I-II),* pp. 521.
57. Sartorio, D.; Tunis, G.; Venturini, S. Nuovi contributi per l'interpretazione geologica e paleogeografica delle Prealpi Giulie (Friuli orientale): il pozzo SPAN1. *Riv. It. Paleont. Strat.* **1987**, *93 (2),* 181-200.
58. 58. Cati, A.; Sartorio, D.; Venturini, S. Carbonate platforms in the subsurface of the northern Adriatic area. *Mem. Soc. Geol. Ital.* **1987**, *40*, 295-308.
59. Tentor, M.; Tunis, G.; Venturini, S. Schema stratigrafico e tettonico del Carso Isontino. *Natura Nascosta* **1994**, *9*, 1-32.
60. Venturini, S. Il pozzo Cargnacco 1: un punto di taratura stratigrafica nella pianura friulana. Mem. Soc. Geol. It. **2002**, 57, 11-18.
61. Sartorio, D.; Tunis, G.; Venturini, S. The Iudrio valley section and the evolution of the northeastern margin of the Friuli Platform (Julian Prealps, NE Italy-W Slovenia). *Mem. Soc. Geol. It.* **1997**, *49*, 163-193.
62. Tunis, G.; Venturini, S. Evolution of the Southern margin of the Julian Basin with emphasis on the megabeds and turbidites sequence of the Southern Julian Prealps (NE Italy). *Geologia Croatica* **1992**, *45*, 127-150.
63. Martinis, B. Ricerche geologiche e paleontologiche nella regione compresa tra il fiume Judrio e il fiume Timavo (Friuli orientale). *Riv. It. Pal. Strat. Mem.* **1962**, *8*, pp. 244.
64. Tunis, G.; Venturini, S. Geologia dei colli di Scriò, Dolegna e Ruttars (Friuli orientale): precisazioni sulla stratigrafia e sul significato paleoambientale del Flysch di Cormons. *Gortania* **1989**, *11*, 5-24.
65. Venturini, S.; Tunis, G. New stratigraphical, paleoenvironmental and tectonic data of the Flysch di Cormons (Eastern Friuli). *Gortania – Atti Museo Friul. Storia Nat*. **1992**, *13*, 5-30.
66. Zanferrari, A.; Avigliano, R.; Monegato, G.; Paiero, G.; Poli, M.E.; Stefani, C. Geological map and explanatory notes of the Geological Map of Italy at the scale 1:50.000: sheet 066 "Udine". *APAT – Servizio Geologico d'Italia – Regione Autonoma Friuli Venezia Giulia* **2008a**. 176 pp., www.isprambiente.gov.it/Media/carg/friuli.html.
67. Stefani, C. Sedimentologia della molassa delle Prealpi Carniche occidentali. *Mem. Soc. Geol. It.* **1984**, *36*, 427-442.
68. Mellere, D.; Stefani, C.; Angevine, C. Polyphase tectonics through subsidence analysis: the Oligo-Miocene Venetian and Friuli Basin, north-east Italy. *Basin Res.* **2000**, *12*, 159-182.
69. Zanferrari, A.; Avigliano, R.; Grandesso, P.; Monegato, G.; Paiero, G.; Poli, M.E.; et al. Geological map and explanatory notes of the Geological Map of Italy at the scale 1:50.000: sheet 065 "Maniago". APAT – Servizio Geologico d'Italia – Regione Autonoma Friuli Venezia Giulia **2008b,** 224 pp., www.isprambiente.gov.it/Media/carg/friuli.html.
70. Fontana, A.; Monegato, G.; Rossato, S.; Poli, M.E.; Furlani, S.; Stefani, C. Carta delle Unità Geologiche della Pianura del Friuli Venezia Giulia alla scala 1:150.000. Regione Autonoma Friuli Venezia Giulia, Direzione centrale ambiente ed energia, Servizio Geologico **2019,** Trieste, Italy.
71. Monegato, G.; Vezzoli, G. Post-Messinian drainage changes triggered by tectonic and climatic events (eastern Southern Alps, Italy). *Sediment. Geol*. **2011,** *239 (3-4),* 188-198, doi:10.1016/j.sedgeo.2011.06.012.
72. Rebez, A.; Cecić, I.; Renner, G.; Sandron, D.; Slejko, D. Misunderstood "forecasts": two case histories from former Yugoslavia and Italy. *Boll. Geof. Teor. Appl*. **2018**, *59,* 481-504, doi: 10.4430/bgta0244.
73. Sandron, D.; Renner, G.; Rebez, A.; Slejko, D. Early instrumental seismicity recorded in the eastern Alps. *Boll. Geofis. Teor. Appl*. **2014**, *55(4),* 755-788, doi: 10.4430/bgta0118.
74. Sitaram, M.V.D.; Borah, P.K. Signal durations and local Richter magnitudes in northeast India: an empirical approach. *J. Geol. Soc. India* **2007**, *70(2),* 323-338.
75. Richter, C.F. Elementary Seismology. W.H. Freeman and Company, San Francisco **1958,** 136-139.
76. Gutenberg, B.; Richter, C.F. Earthquake magnitude, intensity, energy, and acceleration. *Bull. Seismol. Soc. Am.* **1956**, *46(2),* 105-145.
77. Barnaba, P.F. Interpretazione geologico-strutturale della zona di Buja (Friuli). *Mem. Soc. Geol. It*. **1978**, *32*, 4-11.
78. Merlini, S.; Doglioni, C.; Fantoni, R.; Ponton, M. Analisi strutturale lungo un profilo geologico fra la linea Fella-Sava e l'avampaese adriatico (Friuli Venezia Giulia – Italia). *Mem. Soc. Geol. It*. **2002**,57, 293-300.
79. Monegato, G.; Stefani, C. Preservation of a long-lived fluvial system in a mountain chain: the Tagliamento Valley (southeastern Italian Alps). In: Davidson S.K., Leleu S. and North C.P. (eds), From River to Rock Record: The Preservation of Fluvial Sediments and their Subsequent Interpretation, *SEPM Spec. Publ.* **2011**, *97*, 359-374.
80. Ramsay, J. G. Interference Patterns Produced by the Superposition of Folds of Similar Type. (1962). *The Journal of Geology* **1962**, *70 (4),* 466-481. Published By: The University of Chicago Press.
81. Slejko, D.; Neri, G.; Orozova, I.; Renner, G.; Wyss, M. Stress field in Friuli (NE Italy) from fault plane solutions of activity following the 1976 main shock. *Bull. Seismol. Soc. Am*. **1999**, 89, 1037-1052.
82. Álvarez-Gómez, J.A. FMC-Earthquake focal mechanisms data management, cluster and classification. *SoftwareW 9* **2019**, 299-307.
83. Colautti, D.; Finetti, I.; Nieto, D.; Pupis, C.; Russi, M.; Slejko D.; Suhadolc, P. Epicenter distribution and analysis of 1976 earthquakes and aftershocks of Friuli. *Boll. Geof. Teor. Appl*. **1976**, *18*, 457-548.

84. Finetti, I.; Giorgetti, F.; Haessler, H.; Hoang Trong, P.; Slejko, D.; Wittlinger, G. Time space epicenter and hypocenter distribution and focal mechanism of 1976 Friuli earthquakes. *Boll. Geof. Teor. Appl*. **1976**, *18*, 637-655.
85. Cagnetti, V.; Console, R. Space-time distribution of the Friuli (1976) earthquake. *Ann. Geofis.* **1977**, *30*, 107-183.
86. Wittlinger, G.; Haessler, H.; Hoang Trong, P. Contribution to the near field study of the aftershocks of the earthquakes on May 6th and September 15th 1976 in Friuli (Italy). In: *Proc. Spec. Meet. On the 1976 Friuli earthquake and the antiseismic design of nuclear installation* **1978.** CNEN, Roma, Italy, pp. 148-164.
87. Anderson, H.; Jackson, J. Active tectonics of the Adriatic region. *Geophys. J. Int.* **1987**, *91 (3)*, 937-983.
88. 8Ebblin, C. Orientation of stresses and strains in the piedmont area of eastern Friuli, NE Italy. *Boll. Geof. Teor. Appl*. **1976**, *18*, 559-579.
89. Placer, L.; Vrabec; M., Celarc, B. The bases for understanding of the NW Dinarides and Istria Peninsula tectonics. *Geologija* **2010,** *53/1*, 55-86, DOI 10.5474/geologija.2010.005.
90. Venturini, S. Nuovi dati sul Tortoniano del sottosuolo della Pianura Friulana, *Gortania - Atti del Museo Friulano di Storia Naturale* **1987**, *9*, 5-16.
91. Carulli, G.B. Carta geologica del Friuli Venezia Giulia alla scala 1:150000. *Regione Autonoma Friuli Venezia Giulia – Direzione centrale ambiente ed energia – Servizio Geologico* **2006**, S.E.L.C.A. Firenze.
92. Sugan, M.; Renner, G.; Bressan, G.; Restivo, A.; Saraò A. First motion data and focal mechanism solutions of 108 earthquakes occurred between 1928 and 2019 in the Southeastern Alps [Data set], Zenodo, https://doi.org/10.5281/zenodo.4284929, **2020**.
93. Burrato, P.; Poli, M.E.; Vannoli, P.; Zanferrari, A.; Basili, R.; Galadini, F. Sources of MW 5+ earthquakes in north eastern Italy and western Slovenia: an updated view based on geological and seismological evidence. *Tectonophys*. **2008** *453*, 157-176.
94. Venturini, S.; Tunis, G. Nuovi dati ed interpretazioni sulla tettonica del settore delle prealpi Giulie e della regione ai confini fra Italia e Iugoslavia. *Gortania – Atti Museo Friul. Storia Nat.* **1989**, *10*, 5-34.
95. Feruglio E. Le Prealpi fra l'Isonzo e l'Arzino. *Boll. Assoc. Agraria Friuli* **1925**, *s. 7*, 302 pp., Udine.
96. Bosellini, A.; Sarti, M. Geologia del gruppo M. Cuar—M. Covria (Prealpi Carniche). *Giornale di Geologia* **1978,** *43(1)*, 47-88.
97. Ponton, M. Un'area polideformata nelle Prealpi carniche: il Monte Broili e il Cuel dal Meloc. *Gortania – Atti Museo Friulano St. Nat*. **2007**, *28*, 7-18.
98. Ponton, M.; Tunis, G. La geologia del massiccio dei Monti la Bernadia (Prealpi Giulie). In: G. Muscio G. (ed.), Il fenomeno carsico del massiccio dei Monti la Bernadia. *Mem. Ist. Ital. Speleol.* **1996,** *s. II, 8*, 36-48. Udine.
99. Poli, M.E. Il massiccio carbonatico della Bernadia nelle Prealpi Giulie (Friuli, Italia NE): la registrazione di eventi tettonici tra il Cretacico superiore e il Quaternario. *Rendiconti online Soc. Geol. It*. **2008**, *2*, 1-3.
100. Poli, M.E. La carta geologica del Massiccio della Bernadia (Prealpi Giulie meridionali, Friuli, Italia NE). *Rendiconti online Soc. Geol. It*. **2009,** *5*, 168-171.
101. Peruzza, L.; Poli, M.E.; Rebez, A.; Renner, G.; Rogledi, S.; Slejko, D. The 1976-1977 seismic sequence in Friuli: new seismotectonic aspects. *Mem. Soc. Geol. It.* **2002,** *57*, 391-400.
102. Wells, D. L.; Coppersmith, K. J. New empirical relationships among magnitude, rupture length, rupture width, rupture area, and surface displacement. *Bull. Seism. Soc. Am*. **1994**. *84 (4)*, 974-1002.